CHITRAKAR, ROJIN, M.S. Studies of Environmental Pollutant Acrolein-Induced Endothelial Dysfunction: the Role of Glutathione and NF-kappaB. (2015).
Directed by Dr. Zhenquan Jia. 71 pp.

Environmental pollutant exposure has gained considerable attention as a potential risk factor contributing towards cardiovascular diseases (CVDs). Acrolein is a highly reactive electrophilic aldehyde known for its ubiquitous presence in the atmosphere. It is generated during the burning of organic matter and fuels and gets released into the atmosphere through smoke. Acrolein has been studied in the pathology of various respiratory and neurodegenerative disorders. However, the mechanisms regulating the cardiovascular risk implications of acrolein have not been understood completely. The goal of this project was to investigate acrolein-induced cell injury and endothelial dysfunction.

Acrolein, at lower concentrations of 20 and 40 μM, was shown to cause no effect in cellular viability. However, these concentrations of acrolein significantly increased monocyte-endothelial binding through increased expression of monocyte chemoattractant protein-1 (MCP-1), E-selectin, and Interleukin (IL)-8. In addition, acrolein also depleted cellular and mitochondrial glutathione (GSH) and increased the levels of reactive oxygen species (ROS) in endothelial cells. Furthermore, acrolein also induced nuclear factor-kappa B (Nf-kB) transcriptional activity, degradation of inhibitor of kappa B (IkB-α), and nuclear translocation of the p65 subunit.

In contrast, acrolein, at higher concentrations of 80 and 120 μM, was shown to promote EA.hy926 endothelial cell death. In addition, acrolein-incurred cell death at those concentrations was classified to be necrosis, as evidenced by the increased release of lactose dehydrogenase (LDH) and increased staining of DNA-binding propidium iodide (PI). Acrolein also rapidly depleted cellular antioxidant glutathione (GSH) and phase II detoxification enzymes, glutathione-S-transferase (GST) and NAD(P)H Quinone Oxireductase-1 (NQO1), in a dose-dependent manner. To further determine the role of GSH in acrolein-mediated cytotoxicity, we pretreated the cells with buthionine sulfoximine (BSO), an inhibitor for cellular GSH biosynthesis. It was observed that depleted GSH levels significantly potentiated acrolein toxicity. Next, induction of cellular GSH levels, achieved through pre-treatment of endothelial cells with CDDO-Im (1-[2-cyano-3,12 dioxooleana -1,9(11)- dien-28-oyl] imidazolide), was shown to offer cytoprotection against acrolein toxicity. It was also found that the upregulation of GSH by CDDO-Im involved the activation of the Nrf2/ARE signaling and increased expression of the modifier-subunit of γ-glumatylcysteine ligase (GCLM).

In conclusion, acrolein at low concentrations induces monocyte-endothelial interactions, a key step in early atherosclerosis, through depletion of intracellular GSH and activation of Nf-kB pathway. Acrolein at high concentrations induces necrosis in endothelial cells, which can enhance the inflammatory response and increase the susceptibility of developing atherosclerosis. Upregulation of GSH can provide protection against acrolein-mediated cell death. The results, taken together, provide evidence for the

cardiovascular risk posed by acrolein and the importance of GSH and Nf-kB in acrolein toxicity.

Keywords

CVDs, Endothelial dysfunction, Acrolein, GSH, ROS, Nf-kB, Necrosis, Nrf2/ARE

STUDIES OF ENVIRONMENTAL POLLUTANT ACROLEIN-INDUCED ENDOTHELIAL DYSFUNCTION: THE ROLE OF GLUTATHIONE AND NF-KAPPAB

by

Rojin Chitrakar

A Thesis Submitted to
the Faculty of The Graduate School at
The University of North Carolina at Greensboro
in Partial Fulfillment
of the Requirements for the Degree
Master of Science

Greensboro
2015

Approved by

_____
Committee Chair

APPROVAL PAGE

This thesis has been approved by the following committee of the Faculty of The Graduate School at The University of North Carolina at Greensboro.

Committee Chair _____

Zhenquan Jia

Committee Members _____

Olav Rueppell

_____

Yashomati Patel

_____

Date of Acceptance by Committee

_____

Date of Final Oral Examination

ACKNOWLEDGEMENTS

I would like to thank my advisor, Dr. Zhenquan Jia, for his guidance, mentorship, and support. I would also like to thank my committee members, Dr. Olav Rueppell and Dr. Yashomati Patel, for their support and assistance. I would also like to thank Dr. Palanisamy Nallasamy, Halley Shah, Philna Joubert, and the entire Jia lab team for their assistance throughout this project. Finally, I would like to acknowledge the entire University of North Carolina at Greensboro Biology Department for their supportive nature.

TABLE OF CONTENTS

Page

LIST OF FIGURES

Page

CHAPTER I

BACKGROUND

Atherosclerosis

Cardiovascular diseases (CVDs) account for the highest mortality rate for both, men and women, in the United States. Each year, approximately 1.5 million American adults have a heart attack or stroke [1]. In 2010 alone, CVDs accounted for 31.9% of all deaths, or about 1 in every 3 deaths [2]. Most of these CVDs are understood to initiate through a pathological state called atherosclerosis. Atherosclerosis is the build-up of plaques within the arterial walls, narrowing the arterial lumen, and restricting the amount of blood that flows through it. The plaques, formed between the tunica intima and tunica media, are comprised of an accumulation of lipids, cells, debris, and fibrous tissues [3]. In severe cases, the plaques become vulnerable and rupture, attracting coagulant factors in the blood towards the rupture site [3]. With limited blood flow through these clogged arteries, atherosclerosis leads to major complications like heart attack, strokes, and aneurysm [3].

Extensive studies have confirmed that atherosclerosis initiates with endothelial dysfunction. Endothelial cells lineup the inner arterial wall and are essential in maintaining vascular homeostasis, platelet activity, leukocyte adhesion, permeability, and innate immunity [4]. Under the influence of various factors, endothelial cells become activated, making them dysfunctional, which can be characterized with the expression of

adhesion molecules, binding of blood monocytes, and increased permeability and accumulation of circulating lipids [5]. Previous studies have showed that leukocyte binding, facilitated by adhesion molecules and chemokines, is a key step in the development of atherosclerosis [4, 6-9]. The normal endothelial monolayer resists prolonged contact and adhesion to circulating blood monocytes. However, when endothelial cells undergo inflammatory activation, they increase the expression of leukocyte adhesion molecules [10]. Various pro-inflammatory mediators and cell adhesion molecules have been found to be secreted by injured endothelial cells, which include thrombin, tumor necrosis factor-alpha (TNF-α), monocyte chemoattractant protein-1 (MCP-1), Interleukin-8 (IL-8), E-selectin, vascular cell adhesion molecule-1 (VCAM-1), and intracellular adhesion molecule-1 (ICAM-1) [6-9]. Increased production of these cytokines serves as a molecular marker for endothelial inflammation. The adhesion molecules facilitate the recruitment of blood monocytes from the circulation to the endothelium followed by transmigration of the leukocytes to the sub-endothelial [5, 10, 11]. Furthermore, when blood monocytes migrate to the innermost layer of the arterial wall, they differentiate to macrophage foam cells accumulating lipids and lipoprotein particles [10]. These foam cells secrete large amount of TNF-α and other cytokines such as IL-8, E-selectin, which in turn amplify the inflammatory response and enhance vascular complications [10, 11].

Air Pollution-CVD Risk Factor

Many risk factors such as aging, hypercholesterolemia, hyperglycemia, hypertension, and environmental factors have been associated progressively with atherosclerotic development [4]. Among the various environmental factors, air pollution has been gaining a lot of attention as a potential risk factor contributing towards CVDs. Recently, epidemiological studies have demonstrated the association between exposure to air pollution and the risk of developing CVDs [12, 13]. The cardiovascular manifestations resulting from exposure to air pollutants include accelerated atherosclerosis, hypertension, myocardial infarction, and heart failure [14-20]. A few longitudinal studies, involving human subjects, have looked into the association between air pollutants and CVDs. Using thousands of human subjects with no previous record of CVDs, Adar et al. (2013) demonstrated that higher, long-term exposure to particulate matter in air pollution was associated with increased intima-medial thickness (IMT) of the common carotid arteries, an indicator of atherosclerotic progression [21]. Also, numerous animal studies have demonstrated the crucial involvement of air pollutants and particulate matter in atherosclerotic development. For example, exposure to air pollution particulate matter was found to increase the formation and vulnerability of atherosclerotic plaques in rabbits [22, 23]. Although, air pollution has been recognized as an important contributor towards CVDs in humans, its underlying mechanisms remain unclear.

Acrolein: A Common Component of Air Pollution

Acrolein, a highly reactive aldehyde species, is a major air pollutant. It is a pale-yellowish or clear liquid with an acrid, pungent odor [24]. The odor threshold for acrolein is between 0.1 - 0.25 parts acrolein per million parts of air (ppm) [25]. The high vapor pressure of acrolein makes it readily volatile. It can change from liquid to vapor at a faster rate than water at normal temperatures, and its volatility increases with increasing temperatures [24]. It is also highly soluble in water. Therefore, acrolein can be found in air, water, and soil. Commercially, acrolein is used in the production of other chemicals, including acrylic acid. It is also used in pesticides, herbicides, and may also be found in some livestock feed.

Humans are exposed to acrolein every day, particularly through inhalation of smoke, including cigarette smoke. Fujioka and Shibamoto (2006) have reported about 200-500 µg of acrolein per cigarette [26]. Environmental acrolein (about 1/3rd the amount found in cigarettes) corresponds to a wider array of exposure [27]. Acrolein gets released into the atmosphere through incomplete combustion of organic matter like trees and plants and also through burning of fuels like gasoline and diesel. So it is found in all kinds of smoke including cigarette smoke, automobile exhaust, smoke from power plants, furnaces, and fireplaces and even burning foods and oils [25, 27, 28]. With urbanization and increase in air pollution, humans, today, are continuously exposed to acrolein. The US Environmental Protection Agency (EPA) estimates that over 60,000 metric tons of acrolein is emitted annually in the US [24, 27]. Because of its ubiquitous presence, the EPA has classified acrolein as a high-priority air and water toxin [28].

Acrolein has been known to initiate and be a byproduct of lipid peroxidation [28]. Interestingly, it is also produced endogenously in our bodies through the oxidation of lipids and proteins. In that regards, a large body of research has investigated the role of acrolein in the pathogenesis of various neurodegenerative diseases including Alzheimer's disease. Lipid peroxidation in neuronal cells can generate large quantities of acrolein that conjugates with cellular proteins and DNA to form adducts [29, 30]. In addition, the route of human exposure to acrolein, primarily through inhalation, has instigated research focused on implementation of respiratory disease conditions. However, the impact of acrolein on endothelial cells and its role in the development of atherosclerosis has not been well studied. Increased acrolein levels have been reported in atherosclerotic lesions [31], but the mechanism through which acrolein contributes towards atherosclerotic development is not known.

Proposed Study

The primary goal of this proposal is to investigate the role and underlying mechanisms of acrolein in regulation of vascular endothelial dysfunction. We hypothesized that depletion of glutathione (GSH) by exposure to acrolein will increase expression of adhesion molecules and the subsequent endothelial dysfunction, and augmentation of intracellular GSH will ameliorate acrolein-induced toxicity in endothelial cells. Accordingly, the study aims were designed to 1) examine the induction of monocyte adherence to endothelial cells following acrolein treatment and its

underlying mechanisms and 2) examine acrolein-induced endothelial cell death and whether intracellular GSH supplementation could protect against this damage.

CHAPTER II

MECHANISMS OF ACROLEIN-INDUCED MONOCYTE ADHERENCE

Abstract

Acrolein is an unsaturated aldehyde that is predominantly found in smoke and air pollution. It is one of the major toxicants associated with severe health concerns. In this study, we investigated the implications of acrolein in early atherogenesis by examining monocyte adherence to endothelial cells; the mechanisms underlying this atherogenic defining step were also studied. Our results show that acrolein, at concentrations as low as 10 μM, significantly induced monocyte binding to EA.hy926 endothelial cells through increased expression of MCP-1, E-selectin, and IL-8. Acrolein also depleted cellular and mitochondrial GSH and increased the generation of ROS in endothelial cells. Finally, acrolein upregulated the transcriptional activity of genes modulated by βB through degradation of the Nf-kB inhibitor, IkB-α, and increased nuclear translocation of the p65 subunit. These results provide evidence that acrolein augments monocyte binding to endothelial cells, possibly through the Nf-kB pathway.

Introduction

Atherosclerosis is a progressive chronic condition that involves the build-up of plaques within the arterial walls and results in the hardening and narrowing of the arteries. It leads to major complications like myocardial infarction, cerebral infarction,

and aortic aneurysm [5] and has been accounted for over 24% of total deaths in the United States [2]. Numerous studies have indicated that atherosclerosis is a complex, multi-step process and is preceded by endothelial dysfunction [3, 5, 32]. Under the influence of various factors, endothelial cells become activated and impaired resulting in inflammation, increased permeability, vascular lesion, and thrombosis [5, 32]. A key hallmark of atherosclerotic development is the interaction and subsequent binding of the blood monocytes to inflamed endothelium [3, 33]. Various chemotactic cytokines like interleukin-8 (IL-8), monocyte chemoattractant protein-1 (MCP-1) and other leukocyte adhesion molecules like vascular cell adhesion molecule-1 (VCAM-1), intercellular adhesion molecule-1(ICAM-1), and E-selectin facilitate with the firm adhesion of monocytes to endothelial cells. Pro-atherogenic risk factors like oxidized-low density lipoproteins (ox-LDL), fatty acids, tumor necrosis factor-alpha (TNF-α), and angiotensin II have been shown to increase monocyte adherence to endothelium through increased expression of these molecules [11, 34-36]. Higher levels of plasma E-selectin, ICAM-1, and VCAM-1 have also been observed in patients with carotid atherosclerosis and coronary heart diseases compared to control subjects [37]. Once adhered to inflamed sites on the arteries, monocytes transmigrate to the sub-endothelial space, where they engulf accumulating lipids and oxidized-lipoprotein particles, differentiate, and undergo apoptosis to give rise to the lipid-rich core of atherosclerotic plaques [10, 11].

Epidemiological studies have demonstrated association between exposure to air pollution and the risk of developing cardiovascular diseases (CVDs) [12, 13]. *In vitro* studies have also demonstrated that airborne particulate matter, consisting of transition

metals, hydrocarbons, and endotoxins, causes cytotoxicity via oxidative stress [38]. Mixture of several chemicals and toxicants from air pollution particulate matter have also been shown to induce cardiovascular injury and disease progression [22, 23], however specific chemicals that accelerate CVD risk have not been identified. Acrolein, a highly reactive aldehyde, is a major air pollutant. Inhalation of smoke, including cigarette smoke, automobile exhaust, and pollution, is the primary route of human exposure to acrolein. Because of its high reactivity, it is challenging to measure accurate concentrations of acrolein in the atmosphere. Studies have reported less than a few micromolar concentration of acrolein in ambient air [27, 39]. However, in an enclosed setting such as homes, restaurants, and bars, acrolein concentrations can rise up to 20 times the environmental concentration [27]. In addition to its ubiquitous-natured exposure, endogenous generation has resulted in higher concentrations of acrolein aggregated in human tissues and serum. Acrolein concentrations have been reported to be as high as 80 μM in respiratory fluid of smokers and over 180 μM in patients with renal failure [39]. Acrolein adduction has been found to interrupt and alter the regular function of cellular macromolecules and biomolecules, resulting in cellular damage and death [40, 41]. It has also been implicated in pathological conditions involving oxidative stress including neurodegenerative and pulmonary disorders [39, 42]. However, the cardiovascular implications of acrolein have not been studied extensively.

Since monocyte binding is a key aspect of atherosclerotic development, we tested the hypothesis that acrolein exposure activates and recruits monocytes to endothelial cells. We found that acrolein promoted the adhesion of THP-1monocytes to EA.hy926

endothelial cell monolayer by increasing the expression of various adhesion molecules and chemokines, including E-selectin, MCP-1, and IL-8. We also found that the increased expression of these adhesion molecules was regulated by nuclear factor kappa B (Nf-kB) activation and increased levels of reactive oxygen species (ROS).

Materials and Methods

Chemicals

Acrolein (≥95%, GC) was from Sigma chemicals (St. Louis, MO). Dulbecco's Modified Eagle Medium (DMEM), Fetal Bovine Serum (FBS), and Penicillin Streptomycin (Penn Strep) were from Gibco-Invitrogen (Carlsbad, CA). Calcein-AM and SYBR® Green Master Mix were from Life Technologies (Grand Island, NY). Oligonucleotide primers were from Eurofins (Huntsville, AL). Recombinant human TNF-α was from PeproTech (Rockyhill, NJ). TGX™ precast gels and western blot buffers were from Bio-Rad (Hercules, CA). IkB-α, p65 primary antibodies were from Santa Cruz Biotechnology (Santa Cruz, CA) and GAPDH primary antibody was from Cell Signaling Technology Inc. (Danvers, MA) respectively. The FuGENE® HD Transfection Reagent and Dual-Glo® Luciferase Assay System were from Promega (Madison, WI). All other general chemicals were from Sigma-Aldrich (St. Louis, MO).

Cell Culture and Treatment

EA.hy926 endothelial cells were grown in Dulbecco's Modified Eagle Medium (DMEM) supplemented with 10% Fetal Bovine Serum (FBS) and 1% Penicillin Streptomycin (Penn Strep) in cell culture treated flasks at 37°C with 5% CO_2 in a humidified incubator. The culture media was replaced every 2-3 days and cells were passaged around 90% confluence. For acrolein treatment, the cells were grown in cell culture treated petri-dishes under the same conditions. Acrolein was diluted in Medium 199 (M199) supplemented with 2% FBS and 1% Penn Strep. The DMEM media was replaced with the acrolein-diluted M199 media and incubated for different time periods based on the specific assays.

ViaCount Assay

EA.hy926 cells were grown to confluence and treated with acrolein for 24 hours. The cells were harvested through trypsinization and resuspended in PBS. The cells were then mixed with Guava ViaCount Reagent and incubated in the dark for 15 minutes. The stained cell samples were analyzed using the Guava easyCyte™ flow cytometer and cell viability for the treatment groups were expressed relative to an untreated control.

Adhesion Assay

EA.hy926 cells were grown to confluence, followed by acrolein treatment for 6 hours. The cells were washed with serum-free media and calcein-labeled monocytes were added to the cells. Following an hour of incubation, the cells were washed gently with

PBS to remove unbound monocytes. Finally, the fluorescence intensity was measured using the Bio-Tek microplate reader at excitation and emission wavelengths of 496 nm and 520 nm respectively to determine the quantity of bound monocytes as compared to the untreated control.

Quantitative Polymerase Chain Reaction (qRT-PCR)

EA.hy926 cells were grown to confluence and exposed to acrolein for 3 hours. Total RNA from the cells was extracted using the Trizol Reagent. The purity and quantity of the isolated RNA were assessed using the Nanodrop spectrophotometer. The isolated RNA was then reverse transcribed to cDNA. One µl of the amplified cDNA was added to the SYBR® Green real-time PCR master mix along with specific primer sets. The specific primers for E-selectin were forward 5'-AGCCCAGAGCCTTCAGTGTA-3' and reverse 5'-AACTGGGATTTGCTGTGTCC-3', IL-8 were forward 5'-TAGCAAAATTGAGGCCAAGG-3' and reverse 5'-AAACCAAGGCACAGTGGAAC-3', MCP-1 were forward 5'-GCTCAGCCAGATGCAATCAA-3' and reverse 5'-GGTTGTGGAGTGAGTGTTCAAG-3', and GAPDH were forward 5'-CGACCACTTTGTCAAGCTCA-3' and reverse 5'-AGGGGTCTACATGGCAACTG-3'. The reaction cycles were performed in the Applied Biosystems thermal cycler. A total of 40 cycles was performed for each run as following: 95ºC for 15 seconds, 61ºC for 30 seconds, and 72ºC for 30 seconds. Expression of the housekeeping gene, GAPDH, was also acquired to normalize the expression of other target genes. Quantification of gene

expression was determined using the comparative threshold cycle C_T method and expressed as fold-change compared to the untreated control.

ROS Detection Assay

Reactive oxygen species (ROS) were detected using the luminol-dependent-chemiluminescence assay. EA.hy926 cells were harvested and suspended in air saturated complete phosphate buffered saline (cPBS) solution. Aliquots of $5X10^5$ cells, in microcentrifuge tubes, were added with 5 µl of luminol, 5 µl of horseradish peroxidase (HRP), and acrolein. The cell suspension was mixed thoroughly by vortexing and was transferred immediately into white 96-well assay plates. Luminescence intensity of luminol catalyzed by HRP and amplified by ROS was measured in Bio-Tek microplate reader for 30 minutes at 24 second intervals. Integrated chemiluminescence of the various acrolein treatments were expressed as fold-change compared to an untreated control.

Sample Preparation

After acrolein treatment, the treatment media was dumped and the cells were washed with Phosphate Buffered Saline (PBS) twice. The cells were trypsinized with the addition of about 4 mL of trypsin, followed by incubation at 37°C for 3 minutes and collected through centrifugation. The pellet was resuspended in PBS to wash off trypsin and media remnants. The cells were centrifuged again and the pellet was resuspended in 250 µL of sterile tissue lysis buffer. Next, the cells were sonicated 3 times for 15 seconds with a 15 second interval after each sonication. The sonicated cell lysate was centrifuged

again and the supernatant was collected in a new microcentrifuge tube and was used to perform the various antioxidant enzyme assays.

Mitochondrial Extract Preparation

EA.hy926 cells were grown to confluence, followed by acrolein exposure for 24 hours. The cells were harvested through trypsinization, and the pellet was resuspended in Sucrose Buffer (0.25M sucrose, 10mM Hepes, 1mM EDTA) at pH 7.4 with 0.1% BSA. The cell solution was homogenized using a Dounce homogenizer, followed by centrifugation at 1,000 x g for 10 minutes. The supernatant, containing the mitochondrial fraction, was collected in a fresh microcentrifuge tube and was centrifuged again at 10,000 x g for 10 minutes. The mitochondrial pellet was resuspended in 250 µL of sucrose buffer without BSA and was sonicated 3 times for 15 seconds with 15 second intervals after each sonication. Finally, total protein and GSH concentration was measured for the mitochondrial lysate.

Glutathione (GSH) Assay

Cellular and mitochondrial GSH was determined by o-phthalaldehyde (OPT) fluorometric method. EA.hy926 cells, grown to confluence, were exposed to various acrolein concentrations for 24 hours. Ten microliters of the collected cell lysate were incubated with 12.5 µl of 25% meta-phosphoric acid and 0.1% sodium phosphate buffer at pH 8.0 for 10 minutes at 4º C. The sample was centrifuged at 13,000 rpm for 5 minutes, and 10 µl of the resulting supernatant was further incubated with 0.1% OPT in

methanol and 0.1% sodium phosphate buffer for 15 minutes at room temperature in the absence of light. Fluorescence intensity of GSH-OPT was measured by excitation at 350 nm and emission at 420 nm. The sample GSH content was calculated using a GSH standard curve and was expressed as percentage compared to an untreated control.

Nuclear Extract Preparation

Once treated with acrolein, the cells were collected through trypsinization and nuclear proteins were isolated using the EpiQuik Nuclear Extraction Kit as per the manufacturer's protocol. The cytoplasmic protein fraction was also collected for downstream applications.

Total Protein Assay

Ten µL of the sample was diluted in 790 µL of deionized water and 200 µL of Bradford Protein Dye was added to bring the final volume to 1 ml. The solution was mixed thoroughly and sample absorbance at 595 nm was measured to determine the total protein concentration based on the absorbance of a Bovine Serum Albumin (BSA) standard, 1.48 mg/ml.

Western Blot

Total protein concentration of the collected samples was initially measured. The nuclear and cytoplasmic extract for all acrolein treatments were diluted to an equal concentration in Laemmli buffer containing β-mercaptoethanol, heated at 95°C for 5

minutes, and loaded into TGX™ precast gels. After running the gels, the separated proteins were transferred to a nitrocellulose membrane using the Bio-Rad transfer buffer at 80 volts for 2.5 hours. The transfer setup was put in an ice-cold environment to counter the heat produced during the transfer process. The membrane was then blocked in 1% BSA supplemented Tris-buffered saline with 0.05% Tween-20 (TBST) for an hour. The two blotted membrane, containing the nuclear and cytoplasmic proteins each, were incubated with anti-p65 and anti-IkB-α in TBST overnight at 4°C respectively. Unbound antibodies were washed off and the membrane was then probed with horseradish peroxidase-conjugated secondary antibody for an additional hour. The blot was then developed in Super Signal West Pico Chemiluminescent Substrate and protein bands were developed in the Bio-Rad ChemiDoc XRS System. The membrane was then incubated with stripping buffer at 37 ºC for 20 minutes. The membrane was washed with TBST several times and blocked again in 1% BSA supplemented TBST for an additional hour. Finally, the membrane was probed again with anti-GAPDH primary antibodies, and GAPDH protein levels served as loading controls.

Transfection Assay

EA.hy926 cells, grown to about 60% confluence, were cotransfected with 2 µg of Nf-kB-promoter-luciferase reporter vectors and Renilla luciferase control vector using the FuGENE® HD Transfection Reagent following the manufacturer's protocol. Following incubation with the vectors for 24 hours, the cells were treated with 40 µM acrolein for 3 and 6 hours in presence of the transfection media. The transfected cells

were washed with PBS two times and then lysed in a reporter lysis buffer. The lysate solution was repeatedly pipetted to ensure complete lysis of the cells. Firefly luminescence from the reporter vector and renilla luminescence from the control vector were measured in a luminometer using the Dual-Glo® Luciferase Assay Systems following the manufacturer's protocol. The renilla luminescence served as a transfection control and was used to normalize the expression of the Nf-kB reporter vector.

Results

Acrolein-Induced Endothelial Cell Death

We, first, investigated the effect of acrolein on endothelial cell viability. EA.hy926 cells were treated with various concentrations of 20, 40, 80, and 120 µM acrolein for 24 hours and cellular viability was measured by a ViaCount assay. ViaCount dye-stained cells that fall on the right-side of the slanted gate represent dead cells, while cells that fall on the left-side represent viable cells. With all acrolein treatments, there is an increase in the number of cells plotted on the right-side of the gate (Fig. 1B). Panel A represents the percentage of viable cells in each treatment group, and higher concentrations of 80 and 120 µM acrolein show a significant decrease in cellular viability. With regards to the result from the ViaCount assay, we decided to use acrolein concentration of 40 µM and below to perform functional tests relating to cardiovascular risk assessment.

Acrolein-Induced Monocyte Binding to Endothelial Cells

Atherosclerosis and other cardiovascular conditions are dependent on the interaction of blood monocytes to inflamed endothelial cells. To examine the effect of acrolein on endothelial-monocyte binding, we performed an adhesion assay. EA.hy926 cells, treated with 10, 20, and 40 μM concentrations of acrolein for 6 hours, were incubated with calcein-labeled THP-1 monocytes for an additional hour and fluorescence intensity of the bound monocytes was quantified. All investigated concentrations of acrolein significantly increased monocyte adherence to EA.hy926 cells (Fig. 2). The monocyte binding did not follow a dose-dependent pattern, but all acrolein concentrations resulted in an approximate 1.5 fold increase in monocyte adherence compared to an untreated control.

Acrolein-Induced Expression of Adhesion Molecules

The binding of blood monocytes to endothelial cells are mediated by endothelial cell adhesion molecules (ECAMs), and the expression of these surface molecules are altered at inflammatory sites. We used qRT-PCR to examine the expression of various adhesion molecules and cytokines following acrolein treatment. EA.hy926 cells were treated with a single concentration of 20 μM acrolein for 3 hours and mRNA levels of monocyte chemoattractant protein-1 (MCP-1), E-selectin, and Interleukin 8 (IL-8) were determined. The acrolein treatment significantly increased the relative mRNA levels of all three molecules. Approximate increases of 2, 6, and 4.5 fold were observed for MCP-1, E-selectin, and IL-8 respectively (Fig. 3A, 3B, 3C).

Acrolein Increased ROS Levels in EA.hy926 Cells

Increased ROS levels has been implicated in the pathogenesis of cardiovascular and other diseases as well. Here, we wanted to examine if acrolein can induce ROS levels using the luminol-ROS-chemiluminescence assay. Luminol derived chemiluminescence (CL) assay is a highly sensitive method with a comparatively low detection limit. It has been used widely in the detection of ROS, primarily hydrogen peroxide (H_2O_2). EA.hy926 cells were treated with a single concentration of 10 μM acrolein and ROS levels were determined concurrently by measuring the integrated chemiluminescence for 30 minutes at 24 second intervals. Acrolein, at 10 μM concentrations, significantly increased ROS levels in endothelial cells. It resulted in a 2 fold increase in ROS levels in EA.hy926 cells (Fig. 4).

Acrolein Depleted Cellular and Mitochondrial GSH

Glutathione (GSH), specifically mitochondrial GSH, is a key cellular antioxidant that aids in the maintenance of exogenously or endogenously produced ROS. Changes in GSH levels directly correspond to intracellular oxidative imbalance. With regards to the previous finding of increased ROS levels following acrolein treatment, we sought to examine intracellular GSH levels following acrolein exposure. EA.hy926 cells were treated with 10, 20, and 40 μM concentrations of acrolein and total cellular, as well as mitochondrial, GSH levels were determined. Compared to an untreated control, both intracellular and mitochondrial GSH decreased in a dose-dependent manner (Fig. 5A, 5B). Although significant, the mitochondrial GSH did not exhibit a similar depleting

response as the intracellular GSH indicating that prolonged exposure to acrolein may be required to deplete mitochondrial GSH to extremely low levels.

Acrolein-Induced Nf-kB Activation

The Nf-kB transcription factor is activated in various disease states, and it has also been recognized to mediate the expression of adhesion molecules and chemokines during atherosclerotic progression [11, 43]. Here, we used western blotting and transfection assay to determine Nf-kB activation by acrolein in endothelial cells. Western blot analysis showed a significant increase in the protein levels of p65 in the nuclear lysate of EA.hy926 cells, treated with 40 μM acrolein (Fig. 6A). Over time, there was further translocation of the p65 subunit from the cytosol to the nucleus. In accordance with p65 translocation, the protein levels of inhibitor of kappa B (IkB-α) decreased over time with acrolein treatment (Fig. 6B). Furthermore, acrolein also significantly increased the transcriptional activity of Nf-kB over time, as illustrated by an increased luciferase activity for the Nf-kB-reporter plasmid (Fig. 6C). It indicates acrolein increases the expression of Nf-kB-regulated genes.

Discussion

There is strong epidemiological evidence linking air pollution exposure with increased risk of developing CVDs [12, 13, 21]. However, specific chemicals and toxicants, within the air pollution mixture, that contributes significantly towards increased CVD risk have not been identified and studied in detail. In this study, we

examined the early atherogenic impact posed by acrolein, an α, β-unsaturated aldehyde predominantly found in air pollution. Early atherogenesis is a progressively inflammatory process initiated through endothelial dysfunction. Damage to the endothelial monolayer, through endogenous or exogenous factors, results in loss of its function and is characterized by increased permeability, inflammation, expression of adhesion molecules, and increased leukocyte interactions [10, 33]. The interaction of activated endothelial cells with blood monocytes is a hallmark of early atherosclerotic development and has been tested extensively in animal and cellular models. Pro-atherogenic factors like ox-LDL, hypertriglyceridemia, TNF-α, angiotensin II have all been reported to increase monocyte recruitment to endothelial cells *in vitro* [11, 34-36, 44]. Similarly, TNF-α and hypercholesterolemia have also been reported to increase leukocyte interactions to the aortic endothelium in mice [45, 46].Our study was designed to examine the effect of acrolein on monocyte-endothelial interaction by adhesion assay. And we demonstrated that acrolein, at non-lethal concentrations, significantly increased the binding of THP-1 monocytes to EA.hy926 endothelial cells. The results provide evidence for the cardiovascular risk of acrolein exposure.

We further sought to understand the mechanisms underlying acrolein-induced monocyte-endothelial binding, and investigated the involvement of adhesion molecules and chemotactic cytokines aiding the adhesion process. It has been well-documented that the binding of monocytes are facilitated by adhesion molecules and cytokines expressed by activated endothelial cells [3, 32]. Molecules like ICAM-1, VCAM-1, E-selectin, P-selectin, MCP-1, IL-8 have been understood to play a key role in monocyte-endothelial

interactions, and increased levels of these molecules have also been reported in patients with atherosclerosis and CVDs [10, 37]. In this study, we used qRT-PCR to measure the expression of adhesion molecules and found that acrolein treatment significantly increased the mRNA levels of MCP-1, E-selectin, and IL-8.

Several studies have indicated that reactive oxygen species (ROS) can regulate the expression of adhesion molecules. Increased ROS production in endothelial cells has been implicated to induce inflammatory mediators like tumor necrosis factor-alpha (TNF-α), interleukins, VCAM-1, ICAM-1, and P-selectin and subsequently result in endothelial activation and dysfunction [47, 48]. Reactive oxygen species (ROS) are highly reactive and can interact with cellular macromolecules abolishing their functions [49]. In the case of endothelial cells, the loss of function correlates with loss of the anti-inflammatory, anti-coagulant, and impermeability properties making them susceptible for atherogenesis [4]. Changes in the vascular environment and function by oxidants have been understood to accelerate atherosclerotic development [50]. In addition to cellular injury, ROS can alter low-density lipoproteins (LDL) [51]. Oxidation of LDL is also an early step in atherosclerotic development, and Ox-LDL has been studied extensively to be considered as a pro-atherogenic risk factor [35, 51]. In this study, we showed that acrolein can significantly increase ROS levels at low concentrations in endothelial cells, suggesting that acrolein-induced expression of cell surface adhesion molecules might be regulated by ROS.

Although we demonstrate that acrolein can increase cellular ROS, the mechanism through which ROS are produced remains unclear. ROS can be generated through

multiple mechanisms in cells. First, NADPH oxidase is well known to function as a generator of superoxide, especially in leukocytes [52]. It is a membrane-bound enzyme complex that transfers electron from NADPH to molecular oxygen and produces the superoxide anion [48]. ROS produced from activated NADPH oxidase has also been studied in the pathogenesis of atherosclerosis [48]. The increase in ROS observed in this study might be through acrolein-triggered NADPH oxidase activity. Second, the mitochondrial electron transport chain is also an active site for the production of ROS. Leakage of electrons at mitochondrial complex I and complex III has been associated with the production of superoxide [53, 54]. In addition, studies have also demonstrated that disruption of the electron transport chain through mitochondrial damage or blockage of the respiratory complexes can significantly increase ROS production [54]. Acrolein, might also inhibit the mitochondrial electron transport chain to increase ROS production. Finally, low levels of cellular antioxidants have also been implemented to directly increase ROS production [55]. Cellular antioxidants serve as targets for ROS and protect cellular macromolecules by nullifying the effect of ROS. Acrolein is a highly electrophilic molecule and it may directly react with cellular nucleophiles and antioxidants to increase the cells susceptibility to ROS.

GSH is an intracellular tripeptide antioxidant that reacts with ROS and makes them inactive; it is a key molecule essential in maintaining redox homeostasis and protecting cells from oxidative stress [56, 57]. In correspondence with our finding of acrolein-induced ROS levels in endothelial cells, we also examined the effect of acrolein on cellular GSH levels. Acrolein significantly depleted cellular GSH levels, which

correlates with increased ROS production. In addition, we also found that acrolein significantly decreased mitochondrial GSH. Mitochondria are not only involved in the production of ROS from the electron transport chain, but they also serve as a site for damage from ROS, further generating additional ROS. It is well-established that mitochondria have a separate pool of GSH that defends against ROS produced actively during the electron transport chain [55]. In addition, mitochondrial ROS has also been shown to enhance TNF-α-induced expression of E-selectin and VCAM-1 expression [55]. Altogether, these findings suggest that acrolein may have increased ROS levels in endothelial cells by decreasing cellular and mitochondrial GSH, which eventually, may modulate the expression of adhesion molecules and chemokines in endothelial cells. Acknowledging the uncertainty in the mechanism behind acrolein-influenced ROS production, future work could examine the two other mechanisms stated earlier: acrolein-induced activation of NADPH oxidase and acrolein-induced mitochondrial dysfuntion/disruption of the electron transport chain. Future work could also investigate whether induction of intracellular GSH would lead to decreased acrolein-mediated ROS production.

Nuclear factor kappa B (Nf-kB) transcription factor has been implicated in various inflammation-related disease conditions, including atherosclerosis. It regulates the expression of various genes involved in stress, inflammation, proliferation, and apoptosis [58]. Studies have reported that the expression of adhesion molecules involved in monocyte-endothelial interactions are upregulated with Nf-kB activation [11, 43]. In the cytoplasm under normal conditions, Nf-kB is associated with inhibitor of kappa B

(IkB-α). Under the influence of various stimuli, phosphorylation and subsequent degradation of IkB-α releases the Nf-kB p65 subunit, which translocates into the nucleus. The p65 subunit acts as a transcription factor and enhances the expression of proinflammatory mediators, cytokines, and adhesion molecules [58]. Studies have shown that induction of adhesion molecule and cytokine expression by TNF-α is regulated by Nf-kB activation [11, 59]. So as to understand the signaling pathway involved in expression of adhesion molecules and cytokines, we examined whether acrolein could also activate Nf-kB signaling. Western blot analysis showed that acrolein increased the nuclear abundance of the p65 subunit in endothelial cells in a time-dependent fashion. In accordance with the nuclear translocation, acrolein also resulted in degredation of IkB-α in the cytoplasm in a time-dependent manner. We also transfected EA.hy926 cells with Nf-kB promoter containing luciferase vector and observed that the transcriptional activity of the Nf-kB promoter was also significantly increased with acrolein treatment. These results provide concrete evidence for the involvement of the Nf-kB pathway and suggest that acrolein-induced expression of adhesion molecules may be modulated by this signaling pathway. To further specify a causal relationship between acrolein-induced expression of adhesion molecules and Nf-kB activation, future studies could also investigate whether chemical inhibition or siRNA knockdown of Nf-kB could ameliorate acrolein-induced inflammation in endothelial cells.

In summary, this study assesses the risk of acrolein towards endothelial dysfunction. Acrolein significantly decreased cellular and mitochondrial GSH and increased production of ROS. Several studies have reported that ROS can activate the Nf-

kB pathway [58, 60]. In that regard, acrolein also activated the Nf-kB pathway which corresponds to increased expression of adhesion molecules and cytokines and increased monocyte adherence to endothelial cells. Therefore, we postulate that induction of oxidative stress through GSH depletion by acrolein modulates Nf-kB-regulated expression of adhesion molecules and cytokines in endothelial cells (Fig. 7). These findings add to our understanding of the mechanisms involved in acrolein-induced endothelial dysfunction.

CHAPTER III

IMPORTANCE OF GSH IN ACROLEIN-INDUCED CELL DEATH

Abstract

Acrolein, a reactive aldehyde species, gets released into the atmosphere through incomplete combustion of organic matter and burning of fuels. High levels of acrolein are found in cigarette smoke, which is a primary route of human exposure. This study examines the mechanism behind acrolein-induced endothelial cell death and the effects of modulating intracellular antioxidant levels against acrolein cytotoxicity. Since endothelial cell death has been shown to increase the risk of developing atherosclerotic lesions at those sites, understanding the mechanism of acrolein-induced cytotoxicity could provide novel targets for cardiovascular therapies. Acrolein, at 80 and 120 μM concentration, significantly induced necrotic cell death as evidenced by the increased release of LDH and PI staining. It also resulted in a significant depletion of the cellular antioxidant, GSH. We dwelled further into the role of GSH in acrolein-induced endothelial cell death by using BSO, an inhibitor of the cellular GSH biosynthesis pathway, and found that BSO pretreatment significantly reduced cellular viability. Acrolein concentration, as low as 10 μM, demonstrated significant decrease in viability for the BSO pretreated group. To further understand the role of GSH in acrolein cytotoxicity, CDDO-Im was used to upregulate cellular GSH levels. Pretreatment of EA.hy926 cells with CDDO-Im, prior to acrolein exposure, significantly increased viability through activation of the Nrf2

signaling pathway. The results from this study may contribute towards the assessment of cardiovascular risk of human exposure to acrolein and signifies the importance of GSH and Nrf2 signaling in the process.

Introduction

Cardiovascular diseases (CVDs) account for the highest mortality rates in both, men and women, in the United States and across the world as well. Atherosclerosis, a pathological condition that precedes most CVDs, involves the narrowing and hardening of the arteries through extensive buildup of plaques in the arterial walls [10]. Endothelial cell injury is crucial towards the pathogenesis of atherosclerosis. In addition to functioning as a blood barrier, endothelial cells regulate vascular homeostasis, platelet activity, leukocyte adhesion, permeability, and innate immunity [4]. Any damage to the endothelium, sustained through the body's immune response, infection, or other factors, would affect its normal functioning and has been suggested to be a starting point for atherosclerotic development [61, 62]. A high turnover rate of these endothelial cells, including increased cell death and cell proliferation, has been identified as one of the important factors contributing towards atherosclerotic development [61]. The increased turnover rate affects the integrity of the vascular endothelium, exhausts its anti-inflammatory properties, and makes them susceptible towards thrombosis and atherosclerotic plaque development [62, 63]. In addition, characterizing the type of cell death is also essential as variable endpoints can be achieved through each type. Endothelial cell apoptosis has also been studied in the pathophysiology of

atherosclerosis; pro-atherogenic risk factors, such as hyperglycemia, oxidized low density lipoprotein (ox-LDL), and angiotensin II, have all been shown to induce apoptosis in endothelial cells [62, 64]. However, apoptotic cells are cleared up by macrophages limiting the damage from spreading to surrounding tissues. In contrast, necrotic cell death involves the rupture of the plasma membrane and release of intracellular components which can amplify the inflammatory response in the surrounding tissues exacerbating the injury [65].

Epidemiological studies have demonstrated association between exposure to air pollution and the risk of developing CVDs [12, 13]. Studies have shown that diesel exhaust particles caused damage and affected viability in human pulmonary artery endothelial cells [66]. In addition, cigarette smoke condensate at a concentration of 100 μM has been reported to induce necrosis in endothelial cells [67]. However, specific chemicals, within cigarette smoke, that incur such pathological effects have not been identified. Acrolein, a highly reactive aldehyde species, is a major air pollutant and a component of cigarette smoke as well. Fujioka and Shibamoto (2006) have reported about 200-500 μg of acrolein in a single cigarette [26]. Acrolein has been found to induce lung cell death via inflammation and increased oxidative stress [68]. It has also been shown to induce apoptosis in human bronchial epithelial cells through increased generation of cellular oxidants, and modulation of cellular antioxidants ameliorated acrolein cytotoxicity [42]. Since the primary route of human exposure to acrolein is through inhalation, acrolein has been studied in the pathogenesis of various respiratory diseases. However, acrolein-induced endothelial cell death and subsequent cytoprotection

against this damage has not been studied extensively. Such studies would provide an insight towards the cardiovascular risk implications of acrolein exposure, and it could also assist with the identification of therapeutic targets that aid the restoration of a healthy, functional endothelium.

This study examined the cytotoxic mechanisms of acrolein on EA.hy926 endothelial cells. We hypothesized that depletion of GSH will potentiate acrolein-mediated cytotoxicity and augmentation of intracellular GSH will ameliorate acrolein toxicity in endothelial cells. We demonstrated that acrolein significantly induced necrotic cell death at higher concentrations and depleted cellular GSH levels. Furthermore, induction of GSH via the Nrf2 signaling pathway by CDDO-Im afforded cytoprotection against acrolein toxicity in endothelial cells.

Materials and Methods

Chemicals

Acrolein (≥95%, GC) was from Sigma chemicals (St. Louis, MO). Dulbecco's Modified Eagle Medium (DMEM), Fetal Bovine Serum (FBS) and Penicillin Streptomycin (Penn Strep) were from Gibco-Invitrogen (Carlsbad, CA). Annexin V dye and SYBR® Green Master Mix were from Life Technologies (Grand Island, NY). Oligonucleotide primers were from Eurofins (Huntsville, AL). TGX™ precast gels and western blot buffers were from Bio-Rad (Hercules, CA). Nrf2 and GAPDH primary antibodies were from Santa Cruz Biotechnology (Santa Cruz, CA) and Cell Signaling

Technology Inc. (Danvers, MA) respectively. The FuGENE® HD Transfection Reagent and Dual-Glo® Luciferase Assay System were from Promega (Madison, WI). All other general chemicals were from Sigma-Aldrich (St. Louis, MO).

Cell Culture and Treatment

EA.hy926 endothelial cells were grown in Dulbecco's Modified Eagle Medium (DMEM) supplemented with 10% Fetal Bovine Serum (FBS) and 1% Penicillin Streptomycin (Penn Strep) in cell culture treated flasks at 37°C with 5% CO_2 in a humidified incubator. The culture media was replaced every 2-3 days and cells were passaged around 90% confluence. For acrolein treatment, the cells were grown in cell culture treated petri-dishes under the same conditions. Acrolein was diluted in Medium 199 (M199) supplemented with 2% FBS and 1% Penn Strep. The DMEM media was replaced with the acrolein-diluted M199 media and incubated for different time periods based on the specific assays.

MTT Assay

EA.hy926 cells were grown to about 80% confluence in 96-well tissue culture plate. Following incubation of the cells with different concentrations of acrolein for 24 hours, the media was replaced with 0.5% FBS supplemented DMEM containing 0.2mg/ml MTT (3-(4, 5-dimethylthiazolyl-2)-2, 5-diphenyltetrazolium bromide) reagent and the cells were further incubated for 3 hours. A mixture of dimethyl sulfoxide, isopropanol, and deionized water (1:4:5) was added and cells were incubated at room

temperature for 20 minutes in a rotating platform shaker. Finally, the amount of dissolved formazan was quantified by measuring absorbance at 570 nm using the Bio-Tek microplate reader to determine cell viability.

Lactose Dehydrogenase (LDH) Assay

EA.hy926 cells were grown to confluence, followed by acrolein exposure for 24 hours. Treatment media was collected and centrifuged for 5 minutes at 13,000 rcf. The collected supernatant was mixed with pyruvate and NADH and enzymatic activity of the LDH released in the media was determined by measuring absorbance at 320 nm.

Apoptosis/Necrosis Assay

Apoptosis/necrosis was detected with the Invitrogen Dead cell Apoptosis kit following the manufacturer's protocol. EA.hy926 cells were grown to confluence and treated with acrolein for 24 hours. The cells were harvested through trypsinization and washed once with PBS. The cells were stained with Annexin V-FITC and Propidium iodide (PI) in 1X binding buffer and fluorescence was analyzed by excitation at 488 nm and emission at 530 nm in the Guava easyCyte flow cytometer.

Sample Preparation

After acrolein treatment, the treatment media was dumped and the cells were washed with Phosphate Buffered Saline (PBS) twice. The cells were trypsinized with the addition of about 4 mL of trypsin, followed by incubation at 37°C for 3 minutes and

collected through centrifugation. The pellet was resuspended in PBS to wash off trypsin and media remnants. The cells were centrifuged again and the pellet was resuspended in 250 µL of sterile tissue lysis buffer. Next, the cells were sonicated 3 times for 15 seconds with a 15 second interval after each sonication. The sonicated cell lysate was centrifuged again and the supernatant was collected in a new microcentrifuge tube and was used to perform the various antioxidant enzyme assays.

Total Protein Assay

Ten µL of the sample was diluted in 790 µL of deionized water and 200 µL of Bradford Protein Dye was added to bring the final volume to 1 ml. The solution was mixed thoroughly and sample absorbance at 595 nm was measured to determine the total protein concentration based on the absorbance of a Bovine Serum Albumin (BSA) standard, 1.48 mg/ml.

Glutathione (GSH) Assay

EA.hy926 cells were grown to confluence, followed by acrolein exposure for 24 hours. The cell lysate was incubated with meta-phosphoric acid and 0.1% sodium phosphate buffer at pH 8.0 for 10 minutes. The sample was centrifuged at 13,000 rpm for 5 minutes, and the resulting supernatant was further incubated with o-phthalaldehyde (OPT) solution and 0.1% sodium phosphate buffer for 15 minutes. Fluorescence intensity of GSH-OPT was measured by excitation at 350 nm and emission at 420 nm. The sample

GSH content was calculated using a GSH standard curve and expressed as percent change to an untreated control.

Glutathione S-Transferase (GST) Assay

EA.hy926 cells were grown to confluence, followed by acrolein exposure for 24 hours. Fifteen µl of the collected cell lysate was mixed with Tris-HCl buffer at pH 7.5, 1% BSA, 1-Chloro-2,4-dinitrobenzene (CDNB), and 100 mM GSH. GST catalyzes the conjugation of GSH to CDNB, with the product having a strong absorbance at 340 nm. The enzyme activity was determined by following the absorption of the GSH-CDNB conjugate at 340 nm.

NADPH Quinone Oxireductase-1 (NQO1) Assay

EA.hy926 cells were grown to confluence, followed by acrolein exposure for 24 hours. The cell lysate was mixed with Tris-HCl buffer at pH 7.5, NADPH, and Dichlorophenolindophenol (DCPIP). The enzyme activity was determined by following the continuous reduction of DCPIP which leads to decreased absorbance at 600 nm.

Nuclear Extract Preparation

Once treated with acrolein, the cells were collected through trypsinization and nuclear proteins were isolated using the EpiQuik Nuclear Extraction Kit as per the manufacturer's protocol.

Western Blot

Following 100 nM CDDO-Im treatment, the nuclear extract from EA.hy926 cells was diluted in Laemmli buffer containing β-mercaptoethanol, heated at 95°C for 5 minutes, and loaded into TGX™ precast gels. After running the gels, the separated proteins were transferred to a nitrocellulose membrane. The membrane was blotted in 1% BSA for an hour and washed off. The blotted membrane was probed with anti-Nrf2 primary antibodies overnight at 4°C. The membrane was then probed with horseradish peroxidase-conjugated secondary antibody for an hour. The blot was then incubated with the Super Signal West Pico Chemiluminescent Substrate for 5 minutes and protein bands were developed under the Bio-Rad ChemiDoc XRS System. The membrane was incubated in stripping buffer to strip off bound antibodies, washed with Tris-Buffered Saline containing Tween 20 (TBST), and blotted in 1% BSA. The membrane was probed again with anti-GAPDH primary antibodies, and protein levels of GAPDH were used as loading control.

Transfection Assay

EA.hy926 cells, grown to about 60% confluence, were transfected with Firefly luciferase containing plasmid vectors and Renilla luciferase reporter vector using the FuGENE® HD Transfection Reagent in accordance with the manufacturer's protocol. Following transfection, the cells were treated with 100 nM CDDO-Im for 6 hours in presence of the transfection media. The transfected cells were washed with PBS and then lysed in a reporter lysis buffer. Firefly luminescence and renilla luminescence were

measured in a luminometer using the Dual-Glo® Luciferase Assay System in accordance with the provided protocols and as previously described [11]. The renilla luminescence served as a control and was used to normalize the expression of other target vectors.

Quantitative Polymerase Chain Reaction (qRT-PCR)

EA.hy926 cells were grown to confluence and exposed to acrolein for 6 hours. Total RNA from the cells was extracted using the Trizol Reagent. The purity and quantity of the isolated RNA were assessed using the Nanodrop spectrophotometer. The isolated RNA was then reverse transcribed to cDNA. One µl of the amplified cDNA was added to the SYBR® Green real-time PCR master mix along with primer sets specific to Nrf2, GCLC, GCLM, NQO1, and HO. The specific primers for Nrf2 were forward 5'-GCGACGGAAAGAGTATGAGC-3' and reverse 5'-GTTGGCAGATCCACTGGTTT-3', GCLC were forward 5'-ACCATCATCAATGGGAAGGA-3' and reverse 5'-GCGATAAACTCCCTCATCCA-3', GCLM were forward 5'-CTCCCTCTCGGGTCTCTCTC-3' and reverse 5'-ATCATGAAGCTCCTCGCTGT-3', NQO1 were forward 5'-TTACTATGGGATGGGGTCCA-3' and reverse 5'-TCTCCCATTTTTCAGGCAAC-3', HO were forward 5'-TCCGATGGGTCCTTACACTC-3' and reverse 5'-TAAGGAAGCCAGCCAAGAGA-3' and GAPDH were forward 5'-CGACCACTTTGTCAAGCTCA-3' and reverse 5'-AGGGGTCTACATGGCAACTG-3'. The reaction cycles was performed in the Applied Biosystems thermal cycler. A total of 40 cycles were performed for each run as follows: 95ºC for 15 seconds, 61ºC for 30 seconds, and 72ºC for 30 seconds. Expression of the

housekeeping gene, GAPDH, was also acquired to normalize the expression of other target genes. Quantification of gene expression was determined using the comparative threshold cycle C_T method and expressed as fold-change compared to the untreated control.

Results

Acrolein-Induced Endothelial Cell Death

To further confirm acrolein-mediated cell death, we performed the MTT and LDH assay. EA.hy926 cells were treated with 20, 40, 80, and 120 µM concentrations of acrolein for 24 hours and the two aforementioned viability assays were performed to examine acrolein-induced cell death. EA.hy926 cells, treated with acrolein at higher concentrations of 80 µM and 120 µM, showed a significant decrease in cell viability, while lower concentrations of 20 µM and 40 µM did not decrease cell viability. Acrolein at 80 µM and 120 µM significantly increased the release of cellular LDH in the culture media, as detected by the LDH assay (Fig. 8B). The MTT assay also confirmed a decrease in cellular viability at those concentrations (Fig. 8A).

Acrolein Promoted Necrosis in EA.hy926 Cells

The induction of apoptosis/necrosis following acrolein treatment was analyzed by flow cytometric analysis of EA.hy926 cells stained with Annexin V-FITC and PI. Externally translocated phosphotidylserine in apoptotic cells are stained with Annexin V-

FITC while PI enters necrotic cells and binds to DNA. Figure 2A represents double staining plots with Annexin V and PI. The lower left quadrant (Annexin - /PI -) represents viable cell population. The lower right quadrant (Annexin +/PI -) represents apoptotic cell population. The upper right (Annexin +/PI +) and the upper left (Annexin - /PI +) quadrants represent necrotic cell populations. Acrolein treatments significantly increased cell population at the upper two quadrants indicating that acrolein promotes necrosis in endothelial cells. Acrolein treatment of 80 µM and 120 µM significantly increased the number of necrotic cells indicated by the high percentage of cells stained by PI (Fig. 9B).With regards to such finding, we decided to use concentrations of 80 µM and above to perform our mechanistic studies.

Acrolein Depleted Cellular GSH, GST, and NQO1

Glutathione (GSH) is an important cellular antioxidant in animal cells that protects them against oxidative damage from reactive oxygen species (ROS) and free radicals. GST and NQO1 are enzymes that are involved in cellular biotransformation so as to assist with the detoxification and excretion of xenobiotics and endobiotics. The effect of acrolein on GSH, GST, and NQO1 levels were examined using OPT-GSH fluorescence and enzyme kinetic assays respectively. EA.hy926 cells significantly decreased cellular GSH at both acrolein concentrations in a dose-dependent manner (Fig. 10A). Similarly, acrolein also significantly decreased cellular glutathione-S-transferase (GST) and NAD(P)H:quinone oxidoreductase type1 (NQO1) in EA.hy926 cells (Fig. 10B, 10C).

GSH-Dependent Acrolein Toxicity

To determine if acrolein toxicity in EA.hy926 cells was dependent on cellular GSH, we pre-treated the cells with buthionine sulfoximine (BSO) followed by acrolein treatment. BSO inhibits γ-glutamylcysteine ligase, the fundamental enzyme in cellular GSH biosynthesis pathway. First, working concentrations of BSO were tested for toxicity in EA.hy926 cells with a ViaCount assay. Cells, treated with 25 µM and 50 µM concentrations of BSO for 24 hours, did not show a difference in cellular viability, when compared to an untreated control (Fig. 11A). Next, the functionality of BSO to inhibit cellular GSH synthesis was tested. EA.hy926 cells were treated with 25 µM and 50 µM concentrations of BSO for 24 hours and cellular GSH was measured. Figure 11B shows that both 25 µM and 50 µM concentrations of BSO significantly decreased cellular GSH. Hereafter, all other experiments with BSO included a single concentration of 25 µM. To examine whether acrolein toxicity was dependent on GSH, a MTT assay was performed to measure acrolein-induced cell death with or without BSO pretreatment. Cells were pretreated with or without BSO for 24 hours, followed by various concentrations of acrolein in fresh media for another 24 hours. Comparing cellular viability at each individual concentrations of acrolein, the BSO pretreated group had significantly less viable cells than the BSO untreated group (Fig. 11C). In the BSO untreated group, significant decrease in cellular viability was only observed at a higher concentration of 80 µM acrolein, consistent with previous results. However in the BSO pretreated group, significant decrease in cellular viability was observed in concentrations as low as 10 µM acrolein.

Upregulation of Antioxidant Defense by CDDO-Im Protects against Acrolein-Induced Cell Death

Next, we examined the modulatory effects of elevated GSH levels on acrolein cytotoxicity. CDDO-Im, 1-[2-cyano-3-,12-dioxooleana-1,9(11)-dien-28-oyl]imidazoleis, is a synthetic triterpenoid based of naturally occurring oleanolic acids. It has been found to possess anti-inflammatory and antioxidant properties and has been studied extensively as a treatment strategy against cancer [69]. CDDO-Im has been reported to induce cytoprotective genes and protect hepatocytes against aflatoxin-induced tumorigenesis [70]. However, there seems to be a gap in studies examining the cytoprotective capabilities of CDDO-Im on endothelial cell death. We first examined the potential of CDDO-Im to induce antioxidant GSH and phase II detoxification enzymes, NQO1 and GST. All tested concentrations of CDDO-Im increased cellular levels of GSH in a near dose-dependent manner (Fig 12A). CDDO-Im at 100 nM increased cellular GSH by over 1.5 fold. Similarly, CDDO-Im also induced cellular levels of NQO1 in a dose-dependent manner, and the concentration of 100 nM resulted in a 1.5 fold increase in NQO1 (Fig 12B). Cellular GST levels were not altered by CDDO-Im.

To further study whether upregulated levels of GSH and antioxidant defense by CDDO-Im can protect cells against acrolein-induced cell death, we pretreated EA.hy926 cells with 100 nM CDDO-Im for 24 hours followed by acrolein treatment in fresh media and cellular viability was measured using the MTT assay and the ViaCount assay. Comparing cellular viability at each individual concentrations of acrolein, the CDDO-Im pretreated group had significantly more viable cells than the CDDO-Im untreated group

(Fig. 13A). Although both groups, with and without CDDO-Im, exhibited a dose-dependent response to acrolein treatment, the CDDO-Im treated group had significantly higher percent of viable cells at each acrolein concentration. The ViaCount assay also led to similar conclusions (Fig. 13B, 13C); acrolein treatment of 80 μM and 120 μM resulted in a 30% and 45% reduction in endothelial cell viability respectively. However with CDDO-Im pretreatment, cell viability was only reduced by 10% and 20% for the aforementioned concentrations of acrolein. The phase contrast pictures taken under the EVOS xl microscope also showed drastic changes in cell morphology and increased number of dead, floating cells following acrolein treatment in the CDDO-Im untreated group (Fig. 14).

CDDO-Im Mediated Nrf2 Signaling

Activation of nuclear factor-erythroid 2-related factor 2 (Nrf2) has been reported to coordinately upregulate GSH and phase II enzymes *in vitro* [71]. Nrf2, in the cytoplasm, is bound to Keap1 protein. Upon release from Keap1, in response to various stimuli, Nrf2 translocates to the nucleus and binds to antioxidant response element (ARE) in the promoter region of antioxidant genes stimulating their expression. To understand the mechanism behind CDDO-Im-induced GSH and antioxidant defense levels, we first looked into CDDO-Im-induced nuclear translocation of Nrf2 in EA.hy926 cells. Western blot analysis showed increased Nrf2 levels in the nucleus of CDDO-Im treated cells in a time-dependent fashion (Fig. 15A). Then, we looked into Nrf2-ARE binding that enhances cellular antioxidant gene expression. Firefly luciferase plasmid vectors with

ARE inserted in the promoter were transfected into EA.hy926 cells and ARE activity was determined through detection of luminescence intensity. It was observed that transcriptional activity of luciferase increased with both concentrations of CDDO-Im (Fig. 15B), confirming that CDDO-Im stimulates the expression of genes preceded by an ARE promoter. Finally, gene expression of Nrf2, GCLC, GCLM, NQO1, and HO was quantified by qRT-PCR. Nrf2 had slightly increased expression (Fig. 16A), GCLM had a 3-fold increase (Fig. 16C), NQO1 had a 7000-fold increase (Fig. 16D), and HO had a 4-fold increase (Fig. 16E) following CDDO-Im treatment. GCLC did not show a significant increase in expression compared to the untreated control (Fig. 16B).

Discussion

The endothelium plays an important role in regulating vascular homeostasis, and any damage or dysfunction of the endothelium represents early stages of atherogenesis [4]. Endothelial dysfunction, characterized by inflammation and accumulation of lipids and leukocytes in the arterial intima, is the hallmark of early atherosclerosis [4, 10, 11]. When endothelial cells become damaged and subsequently die, it decreases the integrity of the endothelial monolayer, increases vascular permeability, and makes the inner arteries easily accessible for LDL, cholesterol, and leukocytes circulating in the blood. Areas of the vasculature with high endothelial cell turnover, characterized by high endothelial cell death and regeneration, have been identified to be highly permeable to unesterified cholesterol making those sites susceptible for atherosclerotic development [61]. Furthermore, these damaged sites also attract blood platelets, resulting in

thrombogenesis and plaque development [61]. In this study, we have demonstrated that acrolein, a reactive aldehyde species found in cigarette smoke and air pollution, decreased endothelial cell viability at higher concentrations of 80 and 120 μM. Furthermore, acrolein promoted necrotic cell death in endothelial cells at the aforementioned concentrations as evidenced by the increased release of LDH in the culture media and increased number of endothelial cells stained with the DNA-binding PI. The type of endothelial cell death is highly relevant in the case of atherosclerosis. Since atherosclerotic development is understood to be a chronic inflammatory process, necrotic cell death could significantly contribute towards its progression. The lysis of endothelial cell membranes, through necrosis, allows for the release of cellular content and proinflammatory mediators to the surrounding tissues aggravating the inflammatory response and increasing the potential of atherosclerotic development at such sites [65, 67]. The necrotic cell death promoted by acrolein suggests that it could increase the risk of atherogenesis at these damaged sites.

Oxidative damage has been reported to induce cytotoxicity in numerous cell types through various signaling pathways. Oxidative stress is attained due to an imbalance between the cellular oxidant and antioxidant levels. GSH is an important antioxidant molecule that is essential towards maintaining oxidative balance and regulation of cellular metabolic functions including signal transduction, cell proliferation, and apoptosis [56]. GSH depletion alters the thiol redox balance [56, 72], and in endothelial cells, this could lead to the onset of atherosclerotic development. Wedley et al. (2011) demonstrated that GSH knockdown in mice influenced vascular reactivity; it was

associated with compromised nitric oxide (NO) levels that are important in maintaining vascular tone [73]. Studies have also shown that intracellular GSH regulated TNF-α-induced expression of adhesion molecules and monocyte aggregation in endothelial cells [57]. These findings signify the importance of GSH in cardiovascular risk implications and may represent a therapeutic target for the prevention of atherosclerosis and other CVDs. We demonstrated that acrolein depletes intracellular GSH in a dose-dependent manner. This suggests that GSH might be the first line of cellular defense against acrolein toxicity. The exhaustion of the cellular GSH eliminates the cellular defenses and makes the cell susceptible to oxidative damage [57].

To further examine the importance of GSH in acrolein-induced cytotoxicity, we pretreated the cells with BSO to deplete cellular GSH. BSO inhibits γ-glutamyl cysteine ligase, a crucial rate-limiting enzyme in the cellular GSH biosynthesis pathway. We observed significantly increased cell death in BSO-pretreated group for all acrolein treatments. Significant decrease in cell viability was observed at 80 μM for acrolein treatment alone, however with BSO pretreatment, cell viability was significantly decreased at 10 μM acrolein. This provides evidence that depletion of cellular GSH is a crucial focal point in acrolein-induced endothelial cell death. Oxidative balance, maintained by antioxidant GSH, is crucial for various cell functions and changes to this equilibrium, incurred by acrolein, may affect various signaling pathways ultimately affecting cell proliferation and inducing necrosis [40, 57, 74]. Since endothelial cell damage and death is associated with early stages of atherosclerotic progression and

increased susceptibility towards CVDs, alterations in cellular GSH levels could potentially influence the pathogenesis of atherosclerosis and other CVDs.

In addition to GSH, acrolein also significantly depleted cellular GST and NQO1 levels, two phase II enzymes involved in the biotransformation and detoxification of electrophiles and ROS. In this study, we focused solely on GSH and found staggering evidence for its importance in acrolein toxicity in ECs. Future work could examine the roles of GST and NQO1 in acrolein-mediated cytotoxicity and their detoxification of acrolein. In this context, ethacrynic acid and dicoumarol could be used to inhibit cellular GST and NQO1 respectively, in an effort to examine their specific roles in acrolein-induced endothelial cell death.

To further assess the important role of GSH in acrolein-induced cell death, we examined whether increasing cellular GSH levels could protect endothelial cells against acrolein toxicity. To that extent, we used CDDO-Im to induce GSH levels endogenously. CDDO-Im is a synthetic triterpenoid, based of oleanolic acids. Oleanolic acids are natural steroid-like compounds that exist in food, medicinal herbs, and other plants; they have been shown to possess anti-inflammatory, anti-tumorigenic, and anti-hyperlipidemic properties [75]. CDDO-Im is a synthetic derivative of the oleanolic acid designed for higher potency and effectiveness. In this study, CDDO-Im upregulated cellular levels of GSH in a dose-dependent manner. CDDO-Im, at 100 nM concentration, increased GSH by 1.5 fold and was used for pre-treatment of endothelial cells to examine cytoprotection against acrolein toxicity. We observed significantly increased viable cell count in CDDO-Im pretreated group. CDDO-Im pretreatment decreased endothelial cell viability by 10%

and 20% for acrolein treatments of 80 and 120 μM, which is significantly lower compared to the 30% and 45% reduction in viability for acrolein treatment alone. In accordance with the results from the BSO experiment, these results highlight the importance of GSH in maintaining a functioning endothelial monolayer and its protective feature against acrolein toxicity.

The Nrf2/Keap-1/ARE signaling has been suggested to coordinately regulate cellular GSH and other phase II enzymes [76-78]. Nrf2, in the cytoplasm is bound to kelch-like ECH-associated protein-1 (Keap1). Upon release from Keap1, Nrf2 translocates to the nucleus and forms heterodimers with Maf proteins. The complex then binds to antioxidant response element (ARE), in the promoter region of cytoprotective genes, stimulating their expression [71]. Therefore, we examined whether the action of CDDO-Im in endothelial cells followed Nrf2 signaling. We observed an increase in the abundance of Nrf2 in the nucleus of endothelial cells with CDDO-Im treatment. It also increased the transcriptional activity of the ARE promoter in the Dual Glo luciferase assay. We also measured the relative mRNA levels of the catalytic and modifier subunits of γ-glutamyl cysteine ligase (GCLC and GCLM), the rate-limiting enzyme in the GSH biosynthesis pathway. In addition, we also measured Nrf2, NQO1, and HO levels with qRT-PCR. The expression level of Nrf2 itself was slightly increased while expression of the modifier subunit of the γ-glutamyl cysteine ligase (GCLM) was significantly increased by CDDO-Im. These findings suggest that CDDO-Im upregulates cellular GSH levels by increasing the expression of GCLM through Nrf2 signaling. In addition, mRNA levels of NQO1 and HO were also upregulated in endothelial cells following CDDO-Im

treatment. NQO1 and HO are phase II enzymes that respond to stress and are involved in the detoxification process. These results suggest that the cytoprotective feature of CDDO-Im against acrolein toxicity could be from an overall combined effect of antioxidant defense regulated by the Nrf2 signaling pathway while not just GSH alone. However, our GSH inhibition studies demonstrated the importance of GSH in acrolein toxicity. Therefore, we believe that GSH augmentation by CDDO-Im could be a significant factor that contributes towards its protective nature against acrolein-induced endothelial cell death. In this study, we did not examine the direct effect of arcolein on the Nrf2/ARE signaling pathway. Future work could assess how varying concentrations of acrolein affect the nuclear translocation of Nrf2 and transcriptional activity of ARE promoter.

Our results suggest that Nrf2 signaling pathway by CDDO-Im could be a possible therapeutic target against atherosclerosis. Oxidative stress has been implicated in the pathogenesis of cardiovascular diseases, and Nrf2 signaling is associated with the regulation of the cellular antioxidant defense system and phase II detoxification enzymes. Therefore, pharmaceuticals and therapeutics that target and constitutively activate the Nrf2 pathway could provide a solution against atherosclerosis and other CVDs. CDDO-Im, itself, may also be a promising therapeutic agent to protect against atherogenesis induced by oxidants, including acrolein.

In summary, this study provides evidence for the cytotoxic effects of acrolein in endothelial cells. Acrolein induces necrotic cell death at higher concentrations which corresponds to depleted levels of antioxidant GSH in endothelial cells. Furthermore, augmentation of cellular GSH levels via the Nrf2 pathway by CDDO-Im provides

marked protection against acrolein-induced endothelial cell death (Fig. 17). These findings will contribute to understanding the action of acrolein, which is important in the development of strategies for the prevention of acrolein toxicity.

REFERENCES

1. Ritchey, M.D., et al., *Million hearts: prevalence of leading cardiovascular disease risk factors--United States, 2005-2012.* MMWR Morb Mortal Wkly Rep, 2014. **63**(21): p. 462-7.
2. Go, A.S., et al., *Heart disease and stroke statistics--2014 update: a report from the American Heart Association.* Circulation, 2014. **129**(3): p. e28-e292.
3. Galkina, E. and K. Ley, *Immune and inflammatory mechanisms of atherosclerosis (*).* Annu Rev Immunol, 2009. **27**: p. 165-97.
4. Grover-Paez, F. and A.B. Zavalza-Gomez, *Endothelial dysfunction and cardiovascular risk factors.* Diabetes Res Clin Pract, 2009. **84**(1): p. 1-10.
5. Yin, G., et al., *Connexin43 siRNA promotes HUVEC proliferation and inhibits apoptosis induced by ox-LDL: an involvement of ERK signaling pathway.* Mol Cell Biochem, 2014. **394**(1-2): p. 101-7.
6. Pearson, T.A., et al., *Markers of inflammation and cardiovascular disease: application to clinical and public health practice: A statement for healthcare professionals from the Centers for Disease Control and Prevention and the American Heart Association.* Circulation, 2003. **107**(3): p. 499-511.
7. Thompson, S.G., et al., *Hemostatic factors and the risk of myocardial infarction or sudden death in patients with angina pectoris. European Concerted Action on Thrombosis and Disabilities Angina Pectoris Study Group.* N Engl J Med, 1995. **332**(10): p. 635-41.
8. Danesh, J., et al., *C-reactive protein and other circulating markers of inflammation in the prediction of coronary heart disease.* N Engl J Med, 2004. **350**(14): p. 1387-97.
9. Ridker, P.M., et al., *C-reactive protein and other markers of inflammation in the prediction of cardiovascular disease in women.* N Engl J Med, 2000. **342**(12): p. 836-43.
10. Libby, P., *Inflammation in atherosclerosis.* Nature, 2002. **420**(6917): p. 868-74.
11. Nallasamy, P., et al., *Sulforaphane reduces vascular inflammation in mice and prevents TNF-alpha-induced monocyte adhesion to primary endothelial cells through interfering with the NF-kappaB pathway.* J Nutr Biochem, 2014. **25**(8): p. 824-33.
12. Kunzli, N., et al., *Ambient air pollution and atherosclerosis in Los Angeles.* Environ Health Perspect, 2005. **113**(2): p. 201-6.
13. Kunzli, N. and I.B. Tager, *Air pollution: from lung to heart.* Swiss Med Wkly, 2005. **135**(47-48): p. 697-702.
14. Bhatnagar, A., *Cardiovascular pathophysiology of environmental pollutants.* Am J Physiol Heart Circ Physiol, 2004. **286**(2): p. H479-85.

15. Brook, R.D., et al., *Air pollution and cardiovascular disease: a statement for healthcare professionals from the Expert Panel on Population and Prevention Science of the American Heart Association.* Circulation, 2004. **109**(21): p. 2655-71.
16. Brook, R.D., et al., *Particulate matter air pollution and cardiovascular disease: An update to the scientific statement from the American Heart Association.* Circulation, 2010. **121**(21): p. 2331-78.
17. Simkhovich, B.Z., M.T. Kleinman, and R.A. Kloner, *Air pollution and cardiovascular injury epidemiology, toxicology, and mechanisms.* J Am Coll Cardiol, 2008. **52**(9): p. 719-26.
18. Simkhovich, B.Z., M.T. Kleinman, and R.A. Kloner, *Particulate air pollution and coronary heart disease.* Curr Opin Cardiol, 2009. **24**(6): p. 604-9.
19. Fuks, K., et al., *Long-term urban particulate air pollution, traffic noise, and arterial blood pressure.* Environ Health Perspect, 2011. **119**(12): p. 1706-11.
20. Bauer, M., et al., *Urban particulate matter air pollution is associated with subclinical atherosclerosis: results from the HNR (Heinz Nixdorf Recall) study.* J Am Coll Cardiol, 2010. **56**(22): p. 1803-8.
21. Adar, S.D., et al., *Fine particulate air pollution and the progression of carotid intima-medial thickness: a prospective cohort study from the multi-ethnic study of atherosclerosis and air pollution.* PLoS Med, 2013. **10**(4): p. e1001430.
22. Risom, L., et al., *Oxidative DNA damage and defence gene expression in the mouse lung after short-term exposure to diesel exhaust particles by inhalation.* Carcinogenesis, 2003. **24**(11): p. 1847-52.
23. Suwa, T., et al., *Particulate air pollution induces progression of atherosclerosis.* J Am Coll Cardiol, 2002. **39**(6): p. 935-42.
24. United States. Agency for Toxic Substances and Disease Registry. and Syracuse Research Corporation., *Toxicological profile for acrolein*. 2007, U.S. Dept. of Health and Human Services, Public Health Service, Agency for Toxic Substances and Disease Registry,: [Atlanta, Ga.]. p. xix, 176, [30] p.
25. Levels, N.R.C.U.C.o.A.E.G., in *Acute Exposure Guideline Levels for Selected Airborne Chemicals: Volume 8*. 2010: Washington (DC).
26. Fujioka, K. and T. Shibamoto, *Determination of toxic carbonyl compounds in cigarette smoke.* Environ Toxicol, 2006. **21**(1): p. 47-54.
27. Faroon, O., et al., *Acrolein environmental levels and potential for human exposure.* Toxicol Ind Health, 2008. **24**(8): p. 543-64.
28. Syracuse Research Corporation., Clement Associates., and United States. Agency for Toxic Substances and Disease Registry., *Toxicological profile for acrolein*. 2007, [Atlanta, Ga.]: Agency for Toxic Substances and Disease Registry. xi, 145 p.
29. Huang, Y., et al., *Protective effects of caffeic acid and caffeic acid phenethyl ester against acrolein-induced neurotoxicity in HT22 mouse hippocampal cells.* Neurosci Lett, 2013. **535**: p. 146-51.

30. Jia, Z., et al., *Upregulation of cellular glutathione by 3H-1,2-dithiole-3-thione as a possible treatment strategy for protecting against acrolein-induced neurocytotoxicity.* Neurotoxicology, 2009. **30**(1): p. 1-9.
31. Conklin, D.J., et al., *Acrolein generation stimulates hypercontraction in isolated human blood vessels.* Toxicol Appl Pharmacol, 2006. **217**(3): p. 277-88.
32. Hadi, H.A., C.S. Carr, and J. Al Suwaidi, *Endothelial dysfunction: cardiovascular risk factors, therapy, and outcome.* Vasc Health Risk Manag, 2005. **1**(3): p. 183-98.
33. Fenyo, I.M. and A.V. Gafencu, *The involvement of the monocytes/macrophages in chronic inflammation associated with atherosclerosis.* Immunobiology, 2013. **218**(11): p. 1376-84.
34. Wang, Y., et al., *5TNF-alpha and IL-1beta neutralization ameliorates angiotensin II-induced cardiac damage in male mice.* Endocrinology, 2014. **155**(7): p. 2677-87.
35. Chen, C. and D.B. Khismatullin, *Oxidized Low-Density Lipoprotein Contributes to Atherogenesis via Co-activation of Macrophages and Mast Cells.* PLoS One, 2015. **10**(3): p. e0123088.
36. den Hartigh, L.J., et al., *Postprandial VLDL lipolysis products increase monocyte adhesion and lipid droplet formation via activation of ERK2 and NFkappaB.* Am J Physiol Heart Circ Physiol, 2014. **306**(1): p. H109-20.
37. Hwang, S.J., et al., *Circulating adhesion molecules VCAM-1, ICAM-1, and E-selectin in carotid atherosclerosis and incident coronary heart disease cases: the Atherosclerosis Risk In Communities (ARIC) study.* Circulation, 1997. **96**(12): p. 4219-25.
38. Araujo, J.A. and A.E. Nel, *Particulate matter and atherosclerosis: role of particle size, composition and oxidative stress.* Part Fibre Toxicol, 2009. **6**: p. 24.
39. Shi, R., T. Rickett, and W. Sun, *Acrolein-mediated injury in nervous system trauma and diseases.* Mol Nutr Food Res, 2011. **55**(9): p. 1320-31.
40. Kehrer, J.P. and S.S. Biswal, *The molecular effects of acrolein.* Toxicol Sci, 2000. **57**(1): p. 6-15.
41. Faroon, O., et al., *Acrolein health effects.* Toxicol Ind Health, 2008. **24**(7): p. 447-90.
42. Nardini, M., et al., *Acrolein-induced cytotoxicity in cultured human bronchial epithelial cells. Modulation by alpha-tocopherol and ascorbic acid.* Toxicology, 2002. **170**(3): p. 173-85.
43. Boyle, E.M., Jr., et al., *Inhibition of nuclear factor-kappa B nuclear localization reduces human E-selectin expression and the systemic inflammatory response.* Circulation, 1998. **98**(19 Suppl): p. II282-8.
44. Gower, R.M., et al., *CD11c/CD18 expression is upregulated on blood monocytes during hypertriglyceridemia and enhances adhesion to vascular cell adhesion molecule-1.* Arterioscler Thromb Vasc Biol, 2011. **31**(1): p. 160-6.
45. Jia, Z., et al., *Genistein inhibits TNF-alpha-induced endothelial inflammation through the protein kinase pathway A and improves vascular inflammation in C57BL/6 mice.* Int J Cardiol, 2013. **168**(3): p. 2637-45.

46. Stokes, K.Y., et al., *Role of platelets in hypercholesterolemia-induced leukocyte recruitment and arteriolar dysfunction.* Microcirculation, 2006. **13**(5): p. 377-88.
47. Li, J.M. and A.M. Shah, *Endothelial cell superoxide generation: regulation and relevance for cardiovascular pathophysiology.* Am J Physiol Regul Integr Comp Physiol, 2004. **287**(5): p. R1014-30.
48. Ray, R. and A.M. Shah, *NADPH oxidase and endothelial cell function.* Clin Sci (Lond), 2005. **109**(3): p. 217-26.
49. Griendling, K.K. and G.A. FitzGerald, *Oxidative stress and cardiovascular injury: Part I: basic mechanisms and in vivo monitoring of ROS.* Circulation, 2003. **108**(16): p. 1912-6.
50. Wang, J., et al., *Retinol binding protein 4 induces mitochondrial dysfunction and vascular oxidative damage.* Atherosclerosis, 2015. **240**(2): p. 335-344.
51. Perrotta, I. and S. Aquila, *The role of oxidative stress and autophagy in atherosclerosis.* Oxid Med Cell Longev, 2015. **2015**: p. 130315.
52. Babior, B.M., *The NADPH oxidase of endothelial cells.* IUBMB Life, 2000. **50**(4-5): p. 267-9.
53. Murphy, M.P., *How mitochondria produce reactive oxygen species.* Biochem J, 2009. **417**(1): p. 1-13.
54. Moran, M., et al., *Mitochondrial respiratory chain dysfunction: implications in neurodegeneration.* Free Radic Biol Med, 2012. **53**(3): p. 595-609.
55. Chen, K.H., L.M. Reece, and J.F. Leary, *Mitochondrial glutathione modulates TNF-alpha-induced endothelial cell dysfunction.* Free Radic Biol Med, 1999. **27**(1-2): p. 100-9.
56. Aquilano, K., S. Baldelli, and M.R. Ciriolo, *Glutathione: new roles in redox signaling for an old antioxidant.* Front Pharmacol, 2014. **5**: p. 196.
57. Tsou, T.C., et al., *Glutathione regulation of redox-sensitive signals in tumor necrosis factor-alpha-induced vascular endothelial dysfunction.* Toxicol Appl Pharmacol, 2007. **221**(2): p. 168-78.
58. Yadav, U.C. and K.V. Ramana, *Regulation of NF-kappaB-induced inflammatory signaling by lipid peroxidation-derived aldehydes.* Oxid Med Cell Longev, 2013. **2013**: p. 690545.
59. Paria, B.C., et al., *Tumor necrosis factor-alpha induces nuclear factor-kappaB-dependent TRPC1 expression in endothelial cells.* J Biol Chem, 2003. **278**(39): p. 37195-203.
60. Li, N. and M. Karin, *Is NF-kappaB the sensor of oxidative stress?* FASEB J, 1999. **13**(10): p. 1137-43.
61. Choy, J.C., et al., *Endothelial cell apoptosis: biochemical characteristics and potential implications for atherosclerosis.* J Mol Cell Cardiol, 2001. **33**(9): p. 1673-90.
62. Dimmeler, S., C. Hermann, and A.M. Zeiher, *Apoptosis of endothelial cells. Contribution to the pathophysiology of atherosclerosis?* Eur Cytokine Netw, 1998. **9**(4): p. 697-8.

63. Deanfield, J.E., J.P. Halcox, and T.J. Rabelink, *Endothelial function and dysfunction: testing and clinical relevance.* Circulation, 2007. **115**(10): p. 1285-95.
64. Littlewood, T.D. and M.R. Bennett, *Apoptotic cell death in atherosclerosis.* Curr Opin Lipidol, 2003. **14**(5): p. 469-75.
65. Wang, J.H., et al., *Mechanisms involved in the induction of human endothelial cell necrosis.* Cell Immunol, 1996. **168**(1): p. 91-9.
66. Bai, Y., A.K. Suzuki, and M. Sagai, *The cytotoxic effects of diesel exhaust particles on human pulmonary artery endothelial cells in vitro: role of active oxygen species.* Free Radic Biol Med, 2001. **30**(5): p. 555-62.
67. Messner, B., et al., *Apoptosis and necrosis: two different outcomes of cigarette smoke condensate-induced endothelial cell death.* Cell Death Dis, 2012. **3**: p. e424.
68. Sun, Y., et al., *Acrolein induced both pulmonary inflammation and the death of lung epithelial cells.* Toxicol Lett, 2014. **229**(2): p. 384-92.
69. Place, A.E., et al., *The novel synthetic triterpenoid, CDDO-imidazolide, inhibits inflammatory response and tumor growth in vivo.* Clin Cancer Res, 2003. **9**(7): p. 2798-806.
70. Yates, M.S., et al., *Potent protection against aflatoxin-induced tumorigenesis through induction of Nrf2-regulated pathways by the triterpenoid 1-[2-cyano-3-,12-dioxooleana-1,9(11)-dien-28-oyl]imidazole.* Cancer Res, 2006. **66**(4): p. 2488-94.
71. Zhang, H. and H.J. Forman, *Signaling pathways involved in phase II gene induction by alpha, beta-unsaturated aldehydes.* Toxicol Ind Health, 2009. **25**(4-5): p. 269-78.
72. Nunoshiba, T. and K. Yamamoto, *Role of glutathione on acrolein-induced cytotoxicity and mutagenicity in Escherichia coli.* Mutat Res, 1999. **442**(1): p. 1-8.
73. Weldy, C.S., et al., *Glutathione (GSH) and the GSH synthesis gene Gclm modulate vascular reactivity in mice.* Free Radic Biol Med, 2012. **53**(6): p. 1264-78.
74. Luo, J., J.P. Robinson, and R. Shi, *Acrolein-induced cell death in PC12 cells: role of mitochondria-mediated oxidative stress.* Neurochem Int, 2005. **47**(7): p. 449-57.
75. Liu, J., *Pharmacology of oleanolic acid and ursolic acid.* J Ethnopharmacol, 1995. **49**(2): p. 57-68.
76. Shah, H., et al., *Protection of HepG2 cells against acrolein toxicity by 2-cyano-3,12-dioxooleana-1,9-dien-28-imidazolide via glutathione-mediated mechanism.* Exp Biol Med (Maywood), 2014.
77. Liby, K., et al., *The synthetic triterpenoids, CDDO and CDDO-imidazolide, are potent inducers of heme oxygenase-1 and Nrf2/ARE signaling.* Cancer Res, 2005. **65**(11): p. 4789-98.
78. Reisman, S.A., et al., *CDDO-Im protects from acetaminophen hepatotoxicity through induction of Nrf2-dependent genes.* Toxicol Appl Pharmacol, 2009. **236**(1): p. 109-14.

APPENDIX A

FIGURES

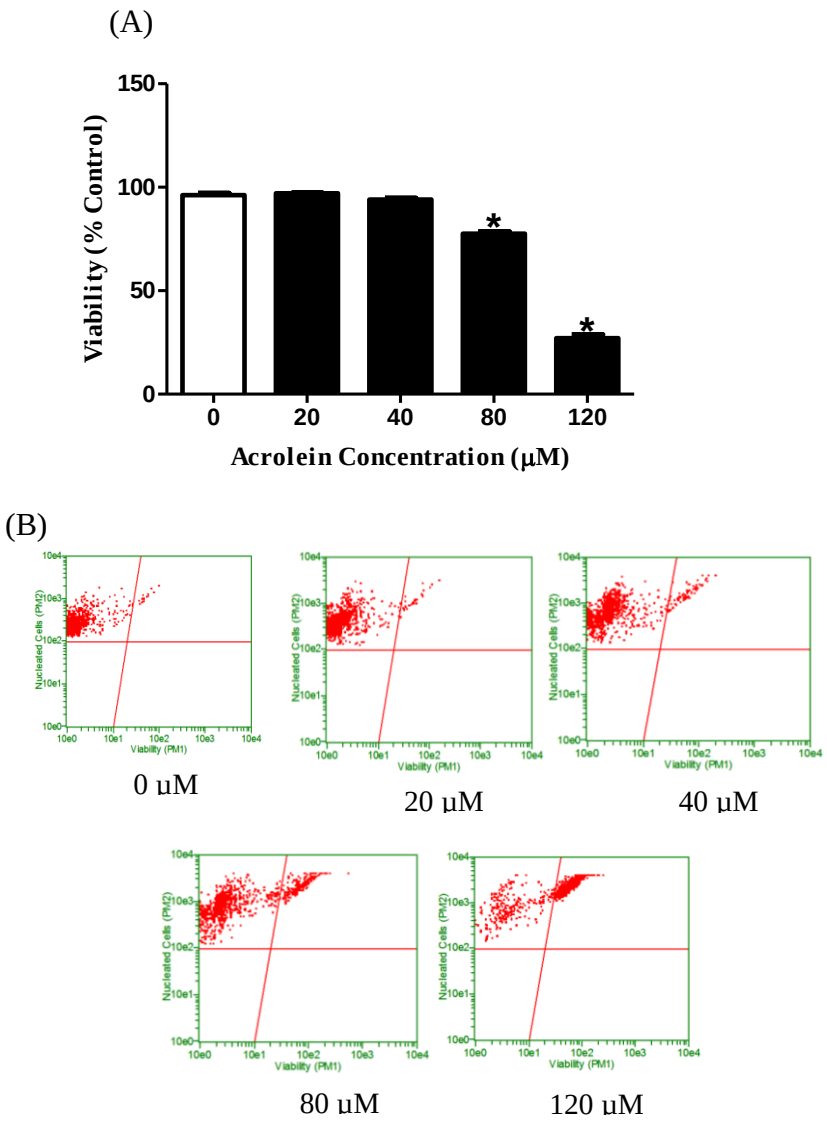

Figure 1. Acrolein-Induced Endothelial Cell Death. *EA.hy926 cells were treated with the aforementioned concentrations of acrolein for 24 hours and cell viability was measured using the ViaCount assay (B). Panel A compares percent viable cells in each treatment groups. Data are mean ± SEM. *P<0.05 compared to control group (n=3).*

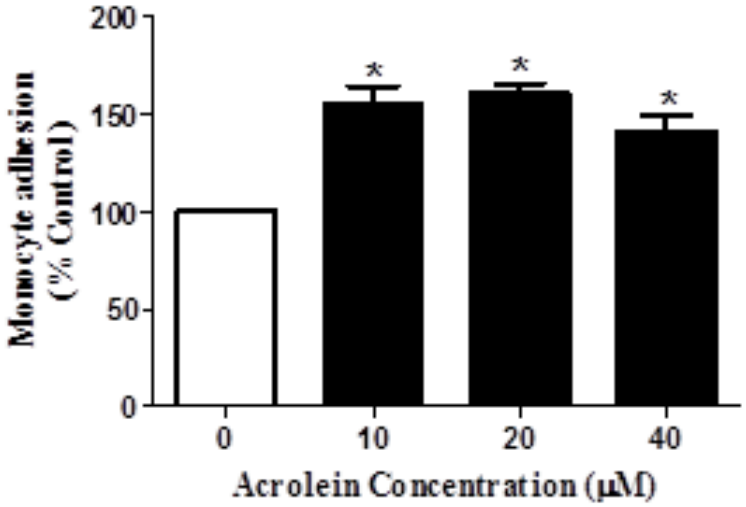

Figure 2. Acrolein-Induced Monocyte Binding to Endothelial Cells. *EA.hy926 cells were treated with the aforementioned concentrations of acrolein for 6 hours. Following treatment, the cells were incubated with fluorescently-labeled THP-1 monocytes for an additional hour and adhesion was quantified by measuring the fluorescence intensity of the bound monocytes. Data are mean ± SEM. *P<0.05 compared to control group (n=3).*

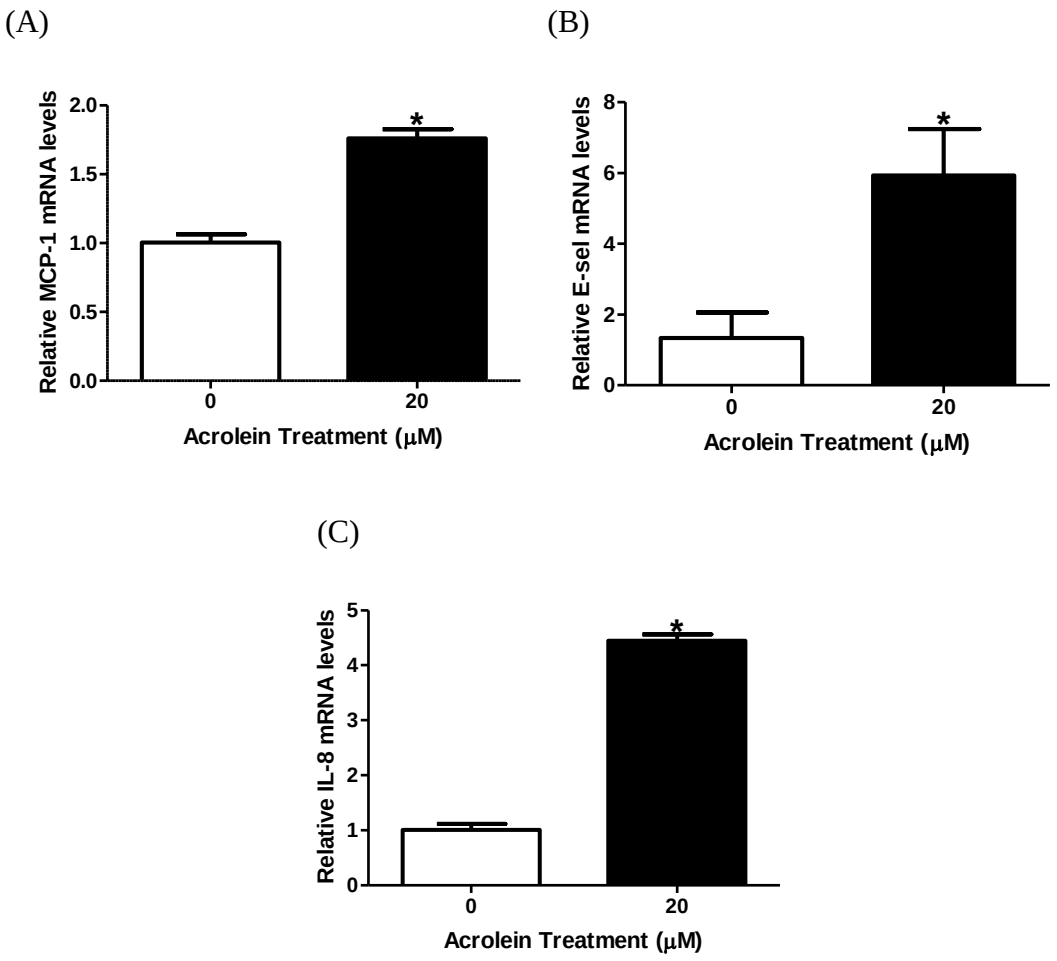

Figure 3. Acrolein-Induced Expression of Adhesion Molecules. *EA.hy926 cells were treated with or without 20 μM acrolein for 3 hours. The mRNA levels of MCP-1 (A), E-selectin (B), and IL-8 (C) were measured by qRT-PCR and normalized to GAPDH expression. Data are mean ± SEM. *P<0.05 compared to control group (n=3).*

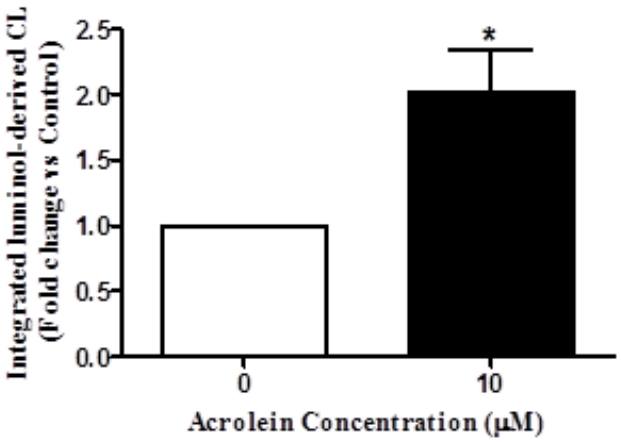

Figure 4. Acrolein-Induced ROS Production in Endothelial Cells. *EA.hy926 cells, suspended in complete phosphate buffered saline (cPBS), were incubated with the 10 µM acrolein, Luminol, and horse-raddish peroxidase (HRP). H_2O_2 levels were determined by measuring the resulting chemiluminescence (CL) of luminol catalyzed by HRP and enhanced by ROS in a plate reader for 30 minutes at 24 second intervals. Data are mean ± SEM. *P<0.05 compared to control group (n=3).*

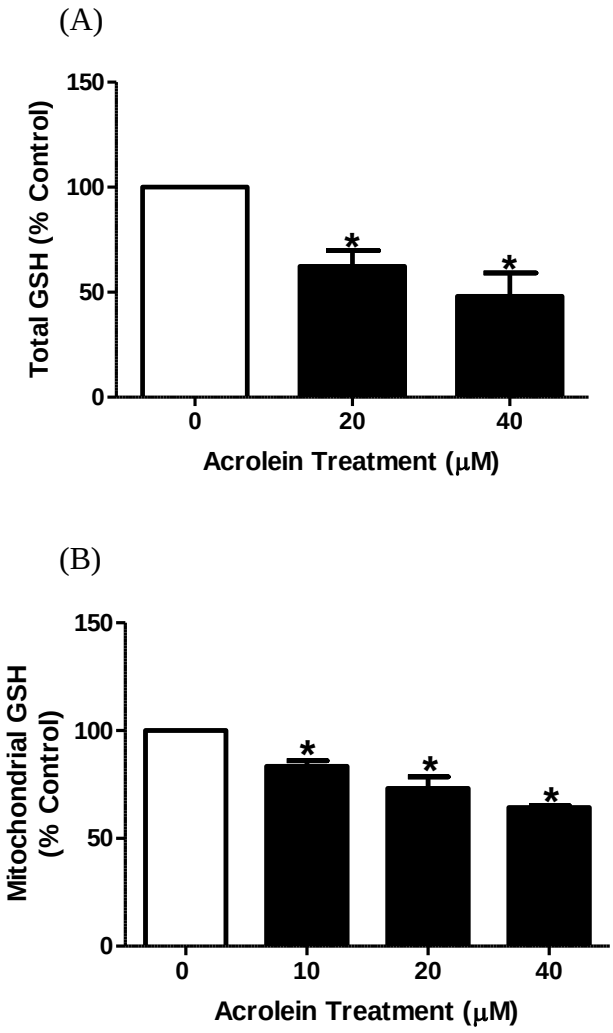

Figure 5. Acrolein Decreased Total Cellular and Mitochondrial GSH*. EA.hy926 cells were treated with various concentrations of acrolein for 24 hours. Total cellular GSH (A) and mitochondrial GSH (B) content were measured fluorometrically with OPT. Data are mean ± SEM. *P<0.05 compared to control group (n=3).*

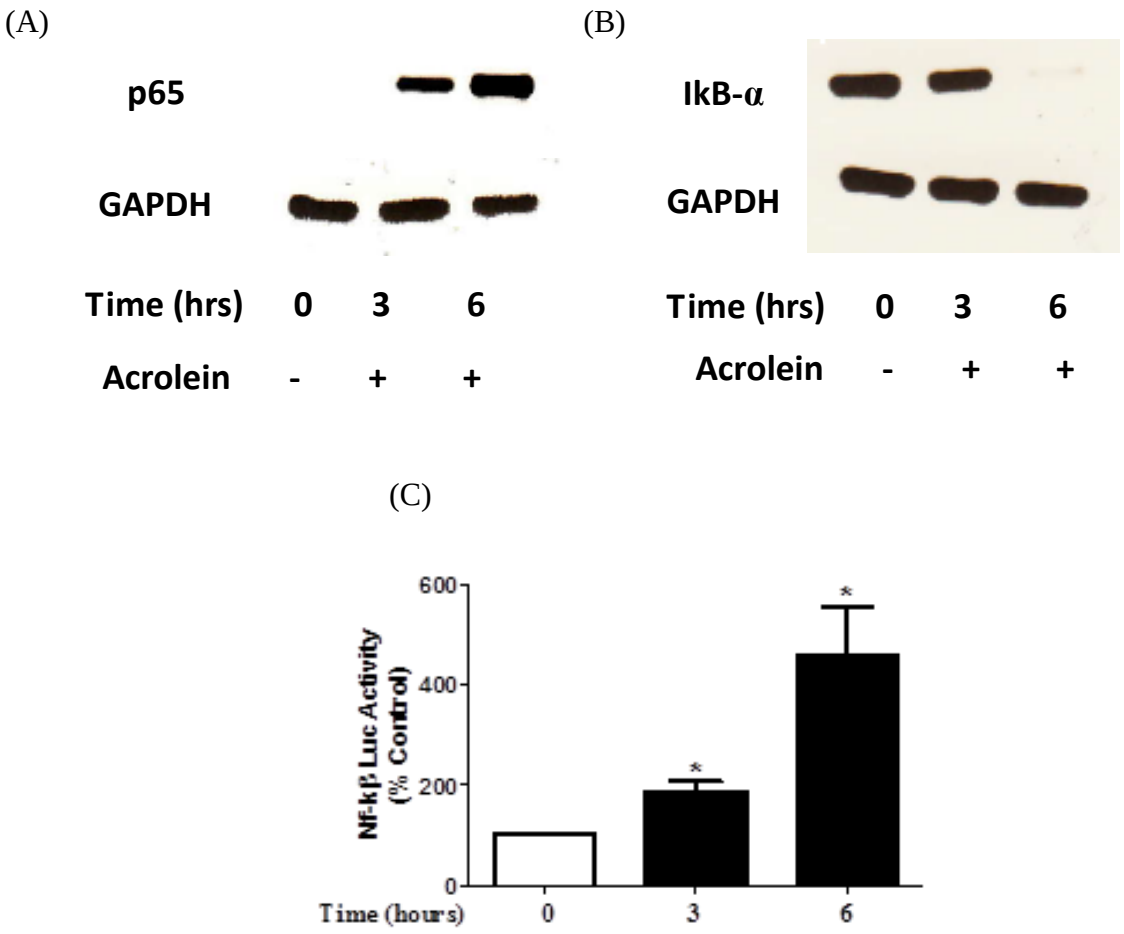

Figure 6. Acrolein-Induced Nf-kB Activation. *EA.hy926 cells were treated with 40 µM acrolein for 3 and 6 hours. The protein levels of p65 (A) in the nuclear lysate and IkB-α (B) in the cytoplasmic lysate were determined by western blotting. GAPDH was used as a loading control. EA.hy926 cells, cotransfected with Nf-kB-luciferase reporter vectors and Renilla luciferase control vectors, were incubated with 40 µM acrolein. Transcriptional activity of Nf-kB was determined by measuring luminescence activity of the reporter vector (C). Nf-kB-luminescence was normalized to Renilla control vector luminescence. Data are mean ± SEM. *P<0.05 compared to control group (n=3).*

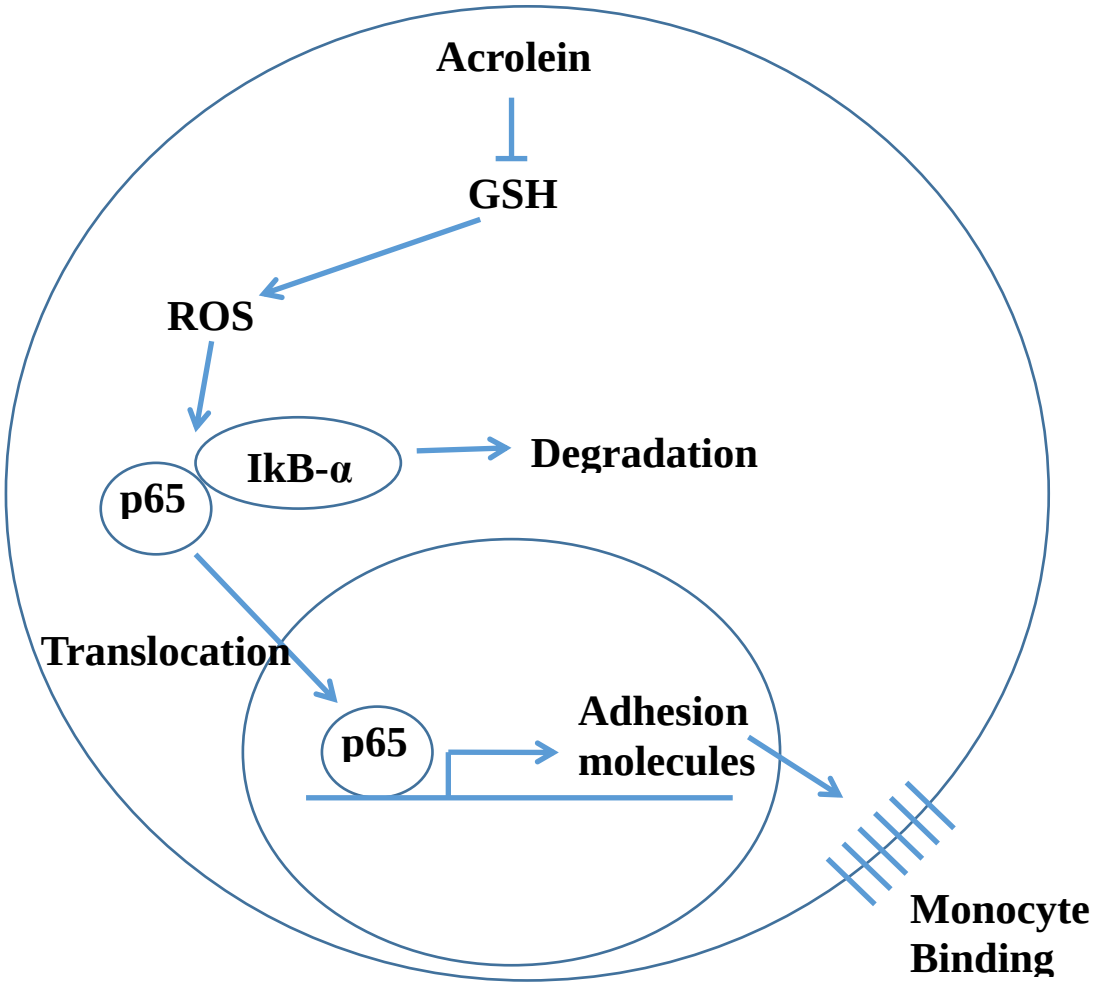

Figure 7. Diagram of Proposed Acrolein-Induced Monocyte Binding to Endothelial Cells.

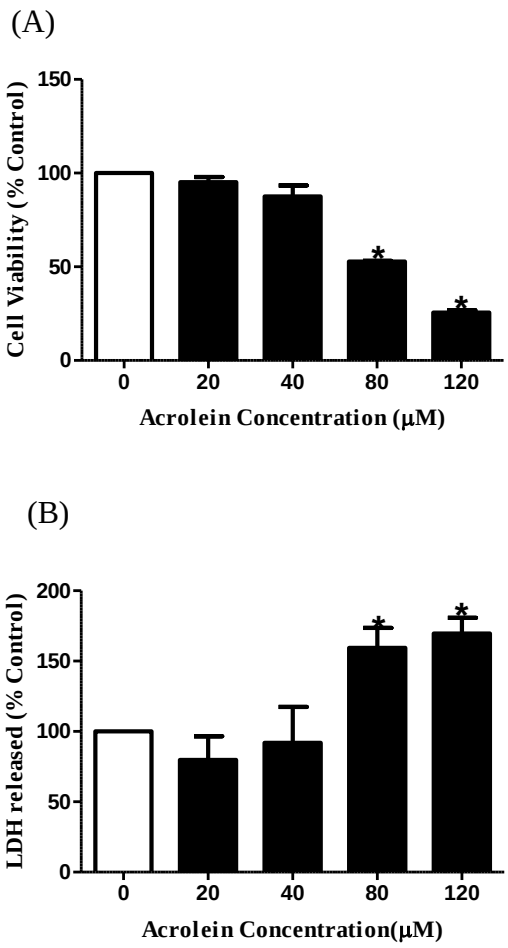

Figure 8. Acrolein-Induced Cytotoxicity in EA.hy926 Endothelial Cells. *EA.hy926 cells were incubated with various concentrations of acrolein for 24 hours and cell viability was determined using the MTT assay (A) and LDH assay (B). Data are mean ± SEM. *P<0.05 compared to control group (n=3).*

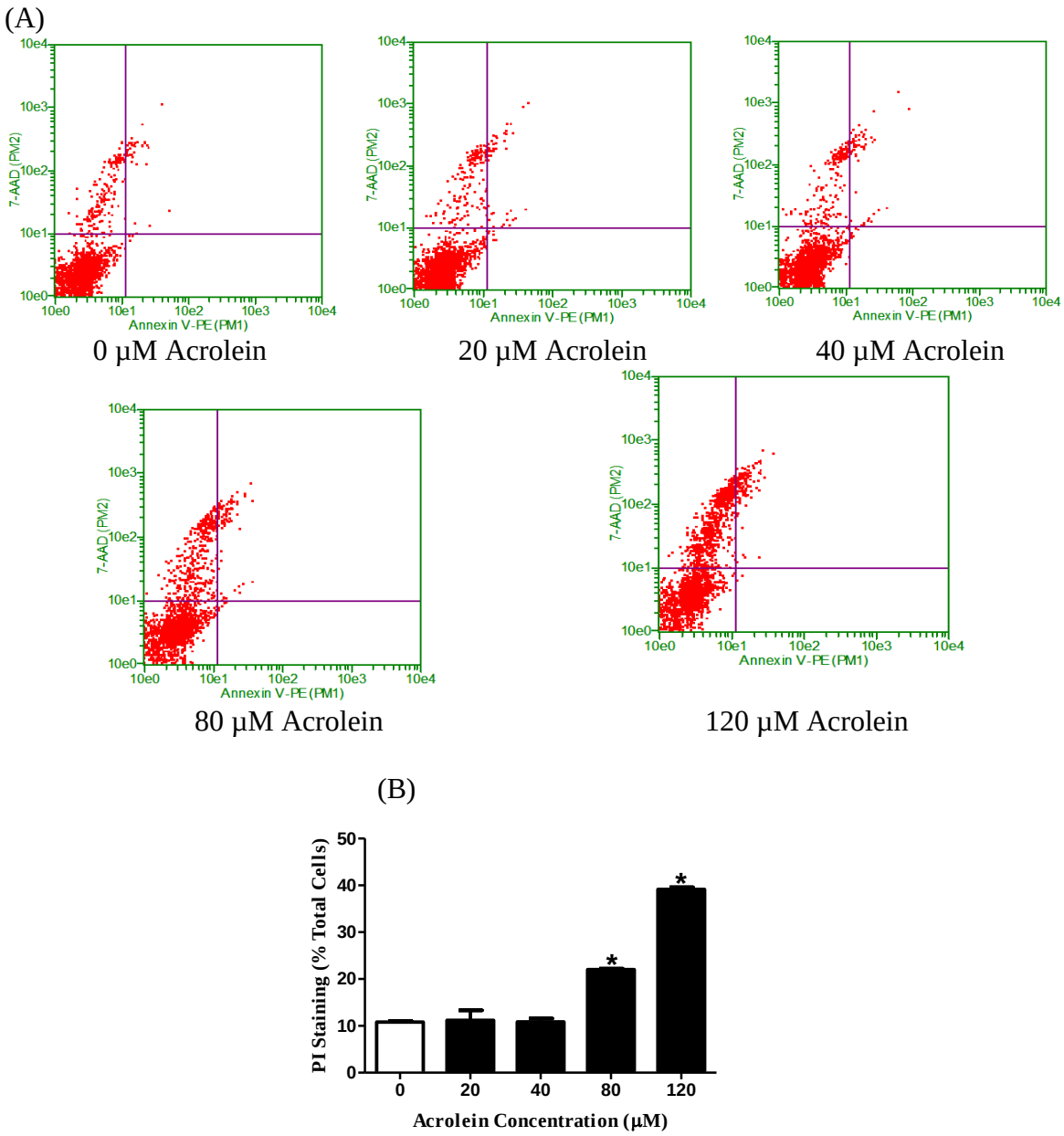

Figure 9. Acrolein-Induced Necrosis. *EA.hy926 cells were treated with the aforementioned concentrations of acrolein for 24 hours. Apoptotic and necrotic cells, stained with Annexin V and PI dye respectively, were detected through flow cytometry. Panel A represents double staining with Annexin V/PI and panel B compares percentage of necrotic cells in each treatment group. Data are mean ± SEM. *P<0.05 compared to control group (n=3).*

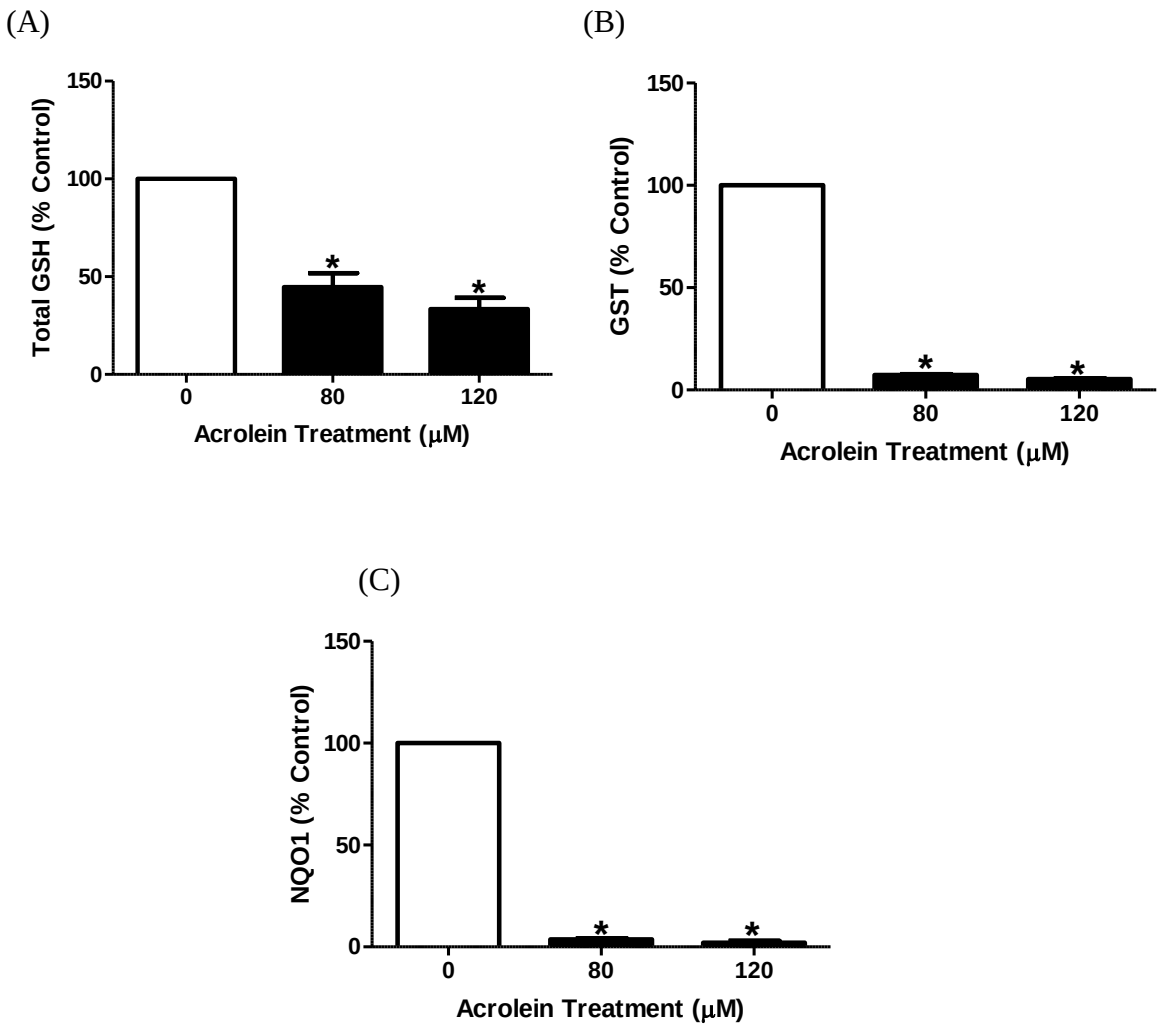

Figure 10. Acrolein Decreased Cellular GSH, GST, and NQO1 in Endothelial Cells. *EA.hy926 cells were treated with various concentrations of acrolein for 24 hours and cellular GSH content was measured fluorometrically with OPT (A). GST activity was measured by following the absorbance of GSH-CDNB conjugate at 340nm (B). NQO1 activity was measured by following the continuous reduction of DCPIP at 600nm (C). Data are mean ± SEM. *P<0.05 compared to control group (n=3).*

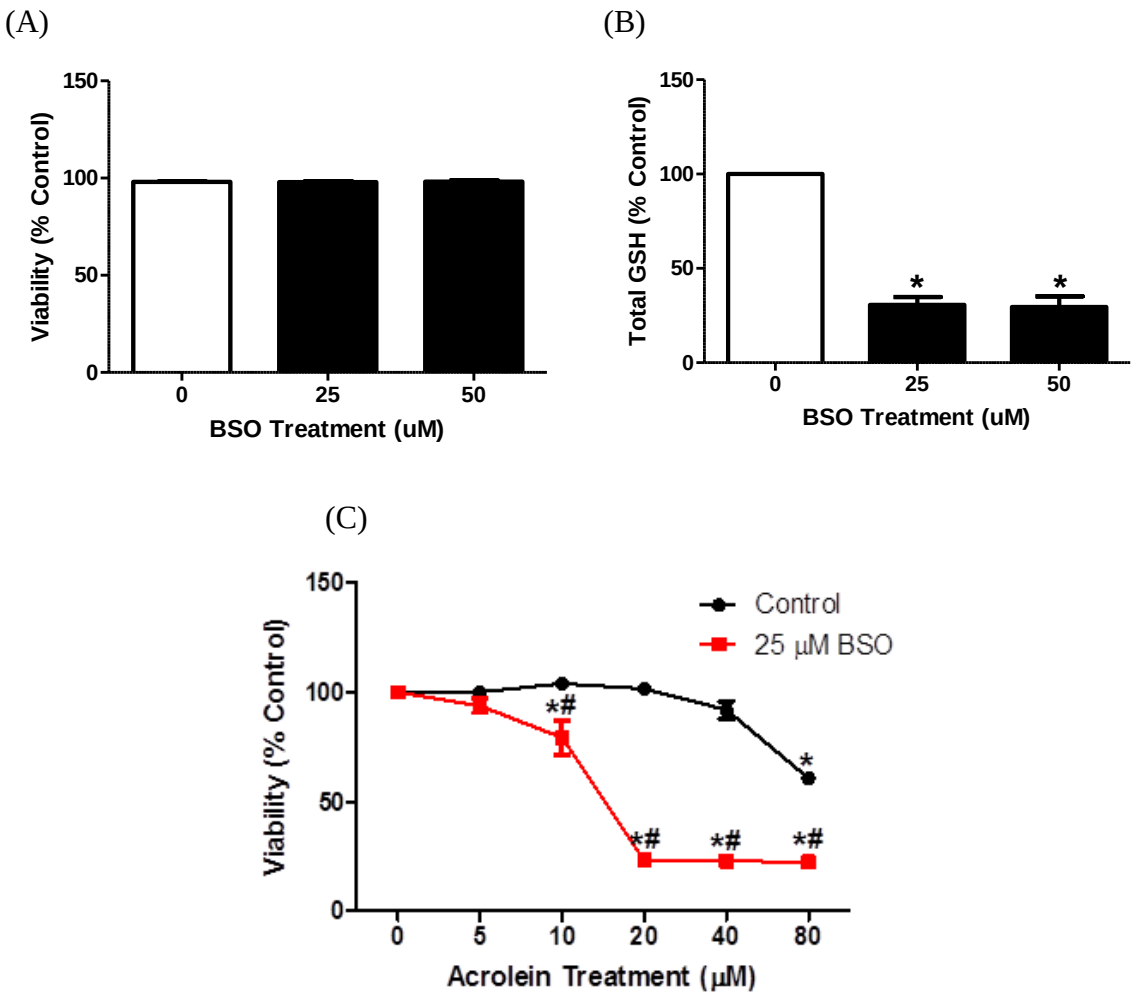

Figure 11. Acrolein Toxicity in EA.hy926 Cells was Dependent on GSH. *EA.hy926 cells were treated with BSO, a chemical inhibitor for GSH biosynthesis, to examine the effect of GSH on acrolein toxicity. Panel A and B depict EA.hy926 cells treated with two concentrations of BSO for 24 hours. Cellular viability and total GSH content were measured using the ViaCount assay and fluorometric detection with OPT respectively. In panel C, EA.hy926 cells were pretreated with or without 25 µM BSO for 24 hours, followed by treatment with the indicated concentrations of acrolein for another 24 hours. Cell viability was measured using the MTT assay. Data represent mean ± SEM. *P<0.05 compared to untreated control (n=3). #P<0.05 compared to the BSO untreated group within the same acrolein treatment (n=3).*

(A)

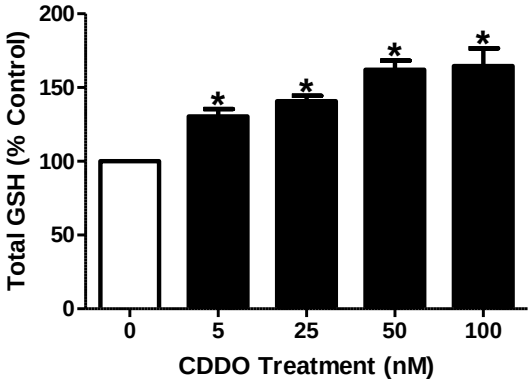

(B)

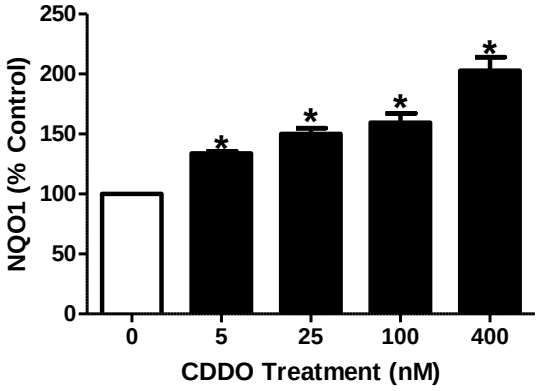

Figure 12. CDDO-Im Induced Cellular GSH and NQO1 Levels. *EA.hy926 cells were treated with the indicated concentrations of CDDO-Im for 24 hours. Total GSH content was measured fluorometrically with OPT (A) and NQO1 activity was measured by following the continuous reduction of DCPIP at 600nm (B). Data represent mean ± SEM. *P<0.05 compared to the control group (n=3).*

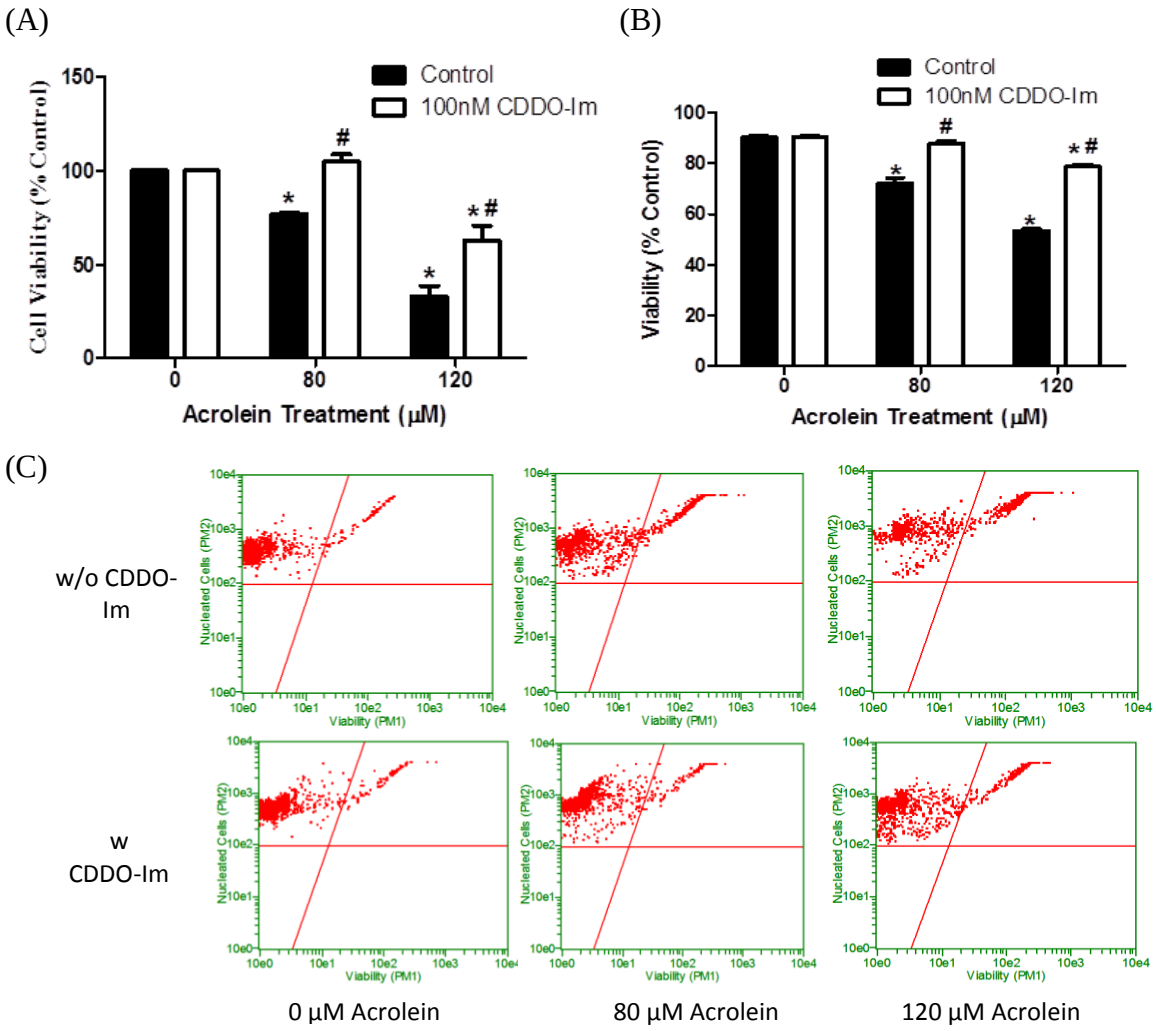

Figure 13. CDDO-Im Protected against Acrolein-Induced Cell Death. *EA.hy926 cells were pretreated with or without 100nM CDDO-Im for 24 hours, followed by treatment with the two mentioned acrolein concentrations for another 24 hours. Cell viability was measured with the MTT assay (A) and the ViaCount assay (C). Panel B compares percent viable cells within and between acrolein treatment groups from the ViaCount assay. Data represent mean ± SEM. *P<0.05 compared to untreated control (n=3). #P<0.05 compared to the CDDO-Im untreated group within the same acrolein treatment (n=3).*

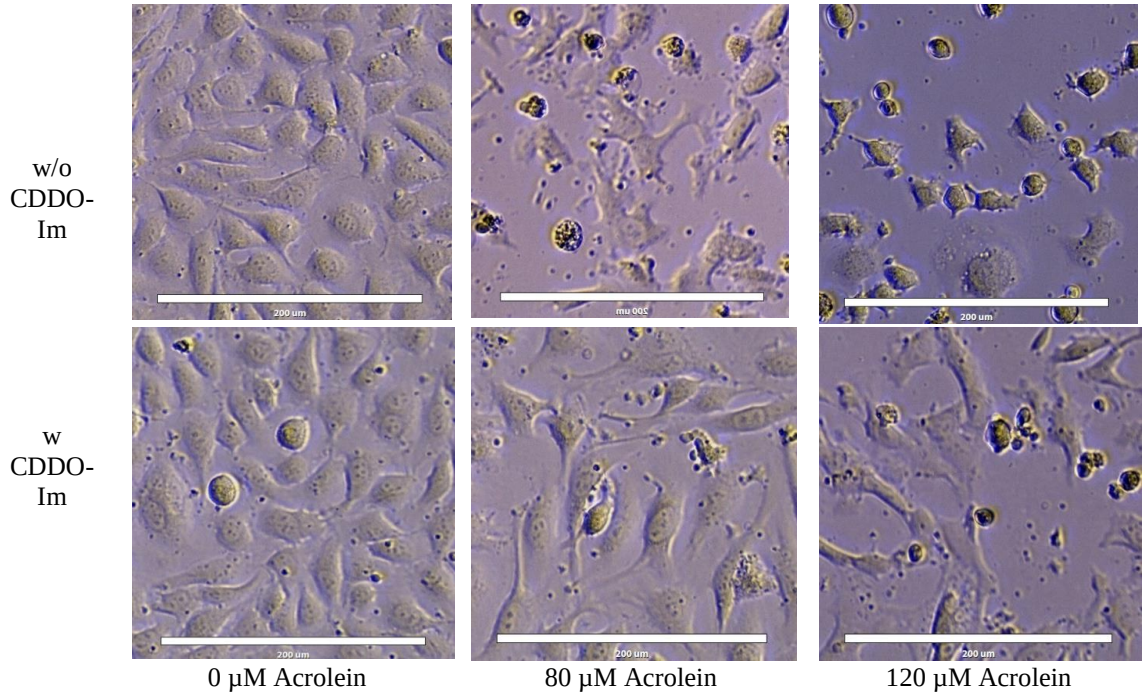

Figure 14. CDDO-Im Protection in Endothelial Cells. *EA.hy926 cells were treated with or without 100 nM CDDO-Im for 24 hours, followed by treatment with the two acrolein concentrations for another 24 hours. Following treatment, phase contrast images were taken under the EVOS xl microscope.*

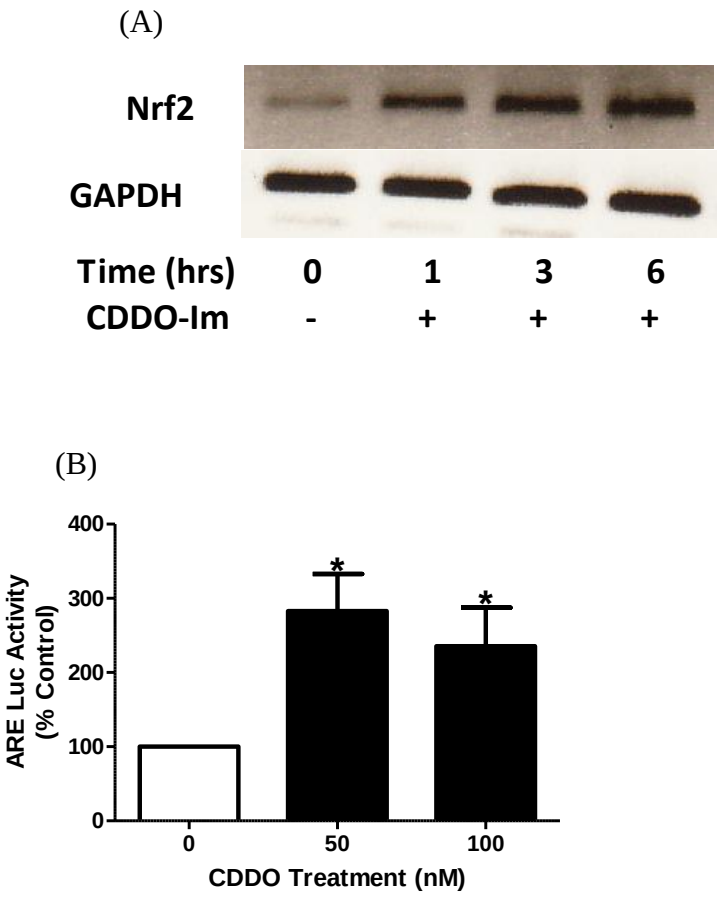

Figure 15. CDDO-Im Mediated Nrf2 Signaling. *EA.hy926 cells were treated with CDDO-Im and Nrf2 protein levels in the nuclear lysate was determined by western blotting (A). GAPDH was used as a loading control. EA.hy926 cells, cotransfected with ARE-luciferase vector and Renilla luciferase control vectors, were incubated with CDDO-Im and luminescence activity was determined (B). ARE-luminescence was normalized to Renilla control vector luminescence. Data represent mean ± SEM. *P<0.05 compared to the control group (n=3).*

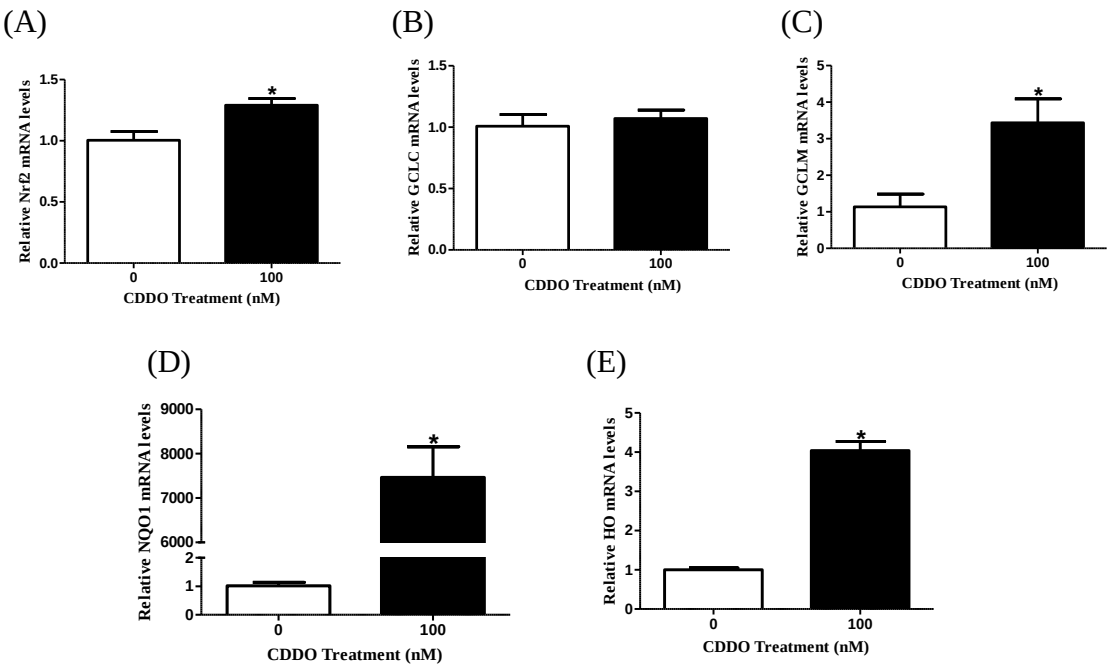

Figure 16. CDDO-Im Induced Nrf2-Mediated Gene Expression. *EA.hy926 cells were treated with 100 nM CDDO-Im for 3 hours and mRNA levels of Nrf2 (A), GCLC (B), GCLM (C), NQO1 (D), and HO (E) were determined using qRT-PCR. GAPDH expression was used to normalize target gene expressions. Data represent mean ± SEM. *P<0.05 compared to the control group (n=3).*

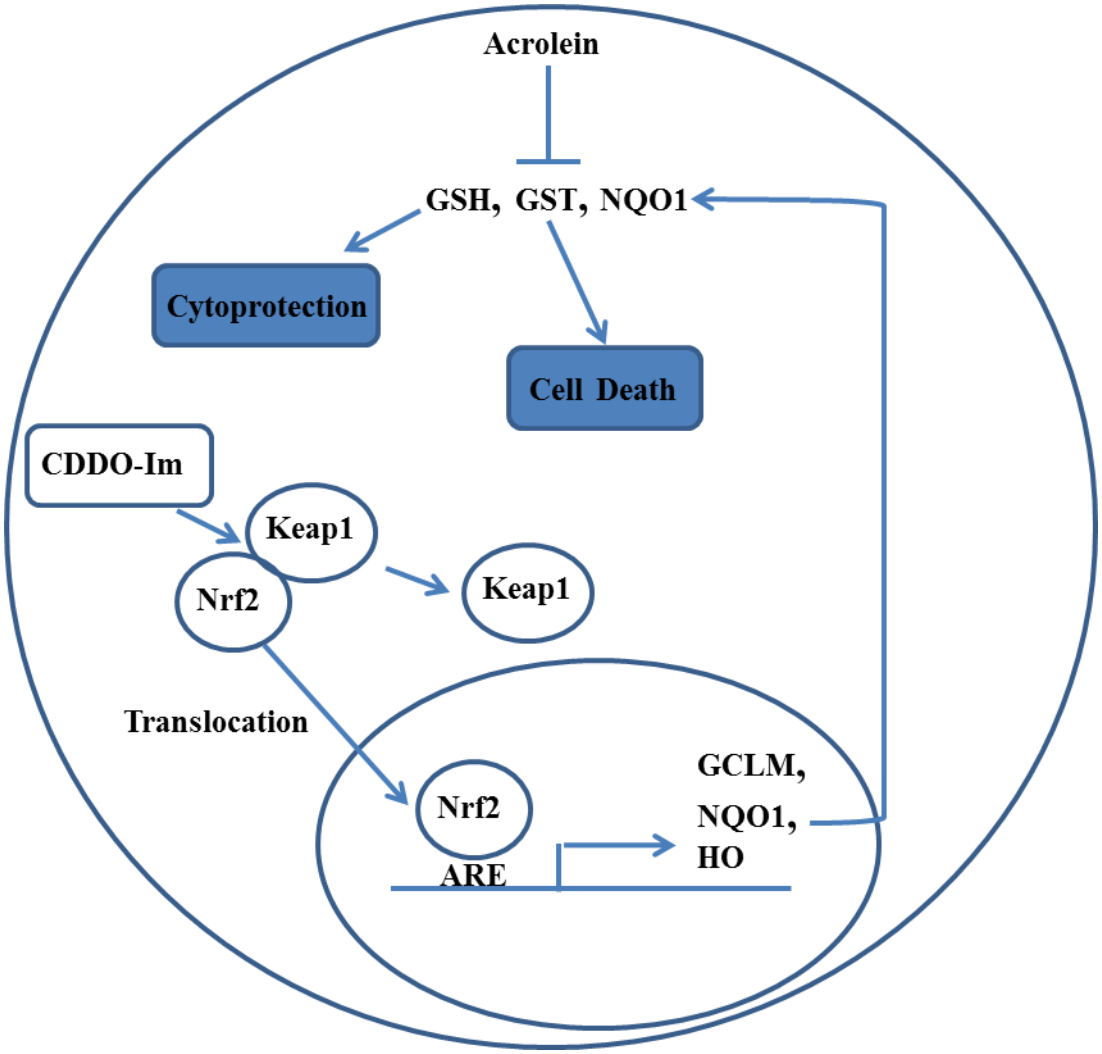

Figure 17. Diagram of Proposed CDDO-Im Mediated Cytoprotection against Acrolein-Induced Cell Death.